MTL TR 91-23

AD

A LAYERED BEAM THEORY FOR SINGLE LAP JOINTS

DONALD W. OPLINGER
MECHANICS AND STRUCTURES BRANCH

June 1991

US ARMY
LABORATORY COMMAND
MATERIALS TECHNOLOGY LABORATORY

U.S. ARMY MATERIALS TECHNOLOGY LABORATORY
Watertown, Massachusetts 02172-0001

The findings in this report are not to be construed as an official Department of the Army position, unless so designated by other authorized documents.

Mention of any trade names or manufacturers in this report shall not be construed as advertising nor as an official indorsement or approval of such products or companies by the United States Government.

DISPOSITION INSTRUCTIONS

Destroy this report when it is no longer needed.
Do not return it to the originator

UNCLASSIFIED

SECURITY CLASSIFICATION OF THIS PAGE (When Data Entered)

REPORT DOCUMENTATION PAGE		READ INSTRUCTIONS BEFORE COMPLETING FORM
1. REPORT NUMBER MTL TR 91-23	2. GOVT ACCESSION NO.	3. RECIPIENT'S CATALOG NUMBER
4. TITLE (and Subtitle) A LAYERED BEAM THEORY FOR SINGLE LAP JOINTS		5. TYPE OF REPORT & PERIOD COVERED Final Report 6. PERFORMING ORG. REPORT NUMBER
7. AUTHOR(s) Donald W. Oplinger		8. CONTRACT OR GRANT NUMBER(s)
9. PERFORMING ORGANIZATION NAME AND ADDRESS U.S. Army Materials Technology Laboratory Watertown, Massachusetts 02172-0001 ATTN: SLCMT-MRS		10. PROGRAM ELEMENT, PROJECT, TASK AREA & WORK UNIT NUMBERS D/A Project: P612105.H84
11. CONTROLLING OFFICE NAME AND ADDRESS U.S. Army Laboratory Command 2800 Powder Mill Road Adelphi, Maryland 20783-1145		12. REPORT DATE June 1991 13. NUMBER OF PAGES 44
14. MONITORING AGENCY NAME & ADDRESS(if different from Controlling Office)		15. SECURITY CLASS. (of this report) Unclassified 15a. DECLASSIFICATION/DOWNGRADING SCHEDULE

16. DISTRIBUTION STATEMENT (of this Report)

Approved for public release; distribution unlimited.

17. DISTRIBUTION STATEMENT (of the abstract entered in Block 20, if different from Report)

18. SUPPLEMENTARY NOTES

19. KEY WORDS (Continue on reverse side if necessary and identify by block number)

Stress analysis
Bonded joints
Structures
Adhesion

20. ABSTRACT (Continue on reverse side if necessary and identify by block number)

(SEE REVERSE SIDE)

DD FORM 1 JAN 73 1473 EDITION OF 1 NOV 65 IS OBSOLETE

UNCLASSIFIED

SECURITY CLASSIFICATION OF THIS PAGE (When Data Entered)

Block No. 20

ABSTRACT

The well known analysis of the single lap joint by Goland and Reissner provided important contributions to the literature on stress analysis of adhesive joints by clarifying not only the importance of adhesive peel stresses in joint failure, but also the role of bending deflections of the joint in controlling the level of the stresses in the adhesive layer. Subsequent efforts have suggested the need for corrections to the Goland and Reissner analysis because of what have been conceived as deficiencies in the model used to describe bending deflections of the central part of the joint where a classical homogeneous beam model without shear or thickness normal deflections were used. The present paper addresses the issue through the use of a more realistic model in which adhesive layer deflections are allowed to decouple the two halves of the joint in the overlap region in the bending deflection analysis, as well as in the analysis of adhesive layer stresses where such a decoupling was allowed by Goland and Reissner. It is found that many of the predictions of the Goland and Reissner analysis are recovered in the limit of large adherend-to-adhesive layer thickness ratios, although substantial differences from the Goland and Reissner analysis can occur for relatively thin adherends.

TABLE OF CONTENTS

NOMENCLATURE

B_U, B_L ($\equiv E't$) -- Stretching stiffness, upper,lower adherend
D_U, D_L ($\equiv E't^3/12$) -- Bending " " " "
E -- Adherend Young's modulus
E' [$\equiv E/(1-\nu^2)$] -- " plane strain Young's modulus
E_b -- Bond Young's modulus
G_b -- " shear "
H_1,H_2 [Eq(37] -- $\Delta_{hj}/\{E'k_{2j}t/2\}$, factors in coefficients of solution for δ_T
J_1,J_2 [Eq(38)] -- H_j divided by roots $U^2/8$ (j=1) and $8\beta^2$ (j=2) of GR solutions
L ($\equiv \ell_o+\ell/2$) -- half length of joint (see Fig. 2)
L (subscript) -- reference to lower adherend
M_U,M_L -- moments in individual adherends
M_o -- moments in loaded adherend at ends of overlap
R -- ratio, U/β
R_j (j=1,2) -- ratios of roots μ_j to $U/(8)^{1/2}$ (j=1) or $(8)^{1/2}\beta$
T_U,T_L -- adherend resultants, $t\sigma_x$
T (x=0,2L) -- resultants applied at ends of joint
U [Eq(A-8)] -- $t(\bar{T}/D_U)^{1/2} \equiv (12\bar{\varepsilon}_x)^{1/2}$
U (subscript) -- reference to upper adherend
$\bar{V}$ -- lateral loads at ends of joint (see Fig. 2)
V_o -- lateral loads at ends of overlap
b (subscript) -- reference to bond layer
c -- $\ell/2$ in GR notation
h -- height (combined thickness) of overlap region in thickness direction
k [Eq(7)] -- ratio of M_o to $\bar{T}t/2$ or of displacement at ends of overlap to t/2
k_{HS} -- k expression obtained by Hart Smith [3]
k_n [Eq(41)] -- k-"new",i.e. k obtained from current analysis
k_{21},k_{22} [Eq(35)] -- ratios of displacement solution coefficients to t/2
ℓ (Fig. 2) -- axial length of overlap region
ℓ_o " " -- axial length of outer section of adherends
t -- adherend thickness
t_b -- bond layer thickness
u -- axial displacement
$\bar{w}$ -- lateral displacement
w_U,w_L -- adherend displacements
$\bar{w}$ [Eq(14.3)] -- $(w_U+w_L)/2$
x -- axial coordinate
z -- thickness-wise coordinate
Δ_{hj} [Eq(22)] -- coefficients of solution of δ_T
β [Eq(A-6.3)] -- $(\rho_G\rho_t)^{1/2}$
δ_T [Eq(14.1)] -- resultant difference T_U-T_L
$\bar{\varepsilon}_x$ -- nominal applied strain, $\bar{\sigma}_x/E'$
γ_b -- bond layer shear strain
λ -- dimensionless overlap length ℓ/t
λ_o -- " length of outer adherend segment ℓ_o/t
μ_1,μ_2 [Eq(22)] -- exponential coefficients of differential equations for $\bar{w}$ and δ_T
ρ_E -- Young's modulus ratio E'/E_b
ρ_G -- modulus ratio E'/G_b
ρ_t -- thickness ration t/t_b

INTRODUCTION

One of the most widely quoted papers in the literature on stresses in adhesive joints is that of Goland and Reissner[1] (subsequently referred to as "GR") on single lap joints. This paper was particularly significant in being the first effort to identify the effects of adherend bending deflections on the peel and shear stresses in the adhesive layer of a single lap joint.

The portion of the GR analysis relating to bending deflections treated the actual joint, Figure 1(A), as a stepped homogeneous beam, Figure 1(B), in which the height of the center section was assumed to be twice the thicknesses of the adherends (thus ignoring the thickness of the bond layer). The forces due to tensile end-loading, assumed to lie along the line a-a' in Figure 1(A), were found to produce varying moment about the neutral axis at any point along the representative beam which resulted in the bending deflections of interest. The deflection analysis for this system was treated essentially by "beam column" analysis [2], i.e. as the analysis of deflections in a beam with combined column (i.e. axial) and lateral loading. (Note that in the GR analysis the column loading is tensile rather than compressive. The latter represents the case used in [2] to introduce the concept of Euler column buckling.)

[1] GOLAND, M. and REISSNER, E., *Stresses in Cemented Joints*, J. Applied Mechanics (ASME), v.11, (1944), p.A17-A27
[2] TIMOSHENKO, S. and GERE, J., *Theory of Elastic Stability*, 2nd ed., Chapt. 1, McGraw Hill (1961)

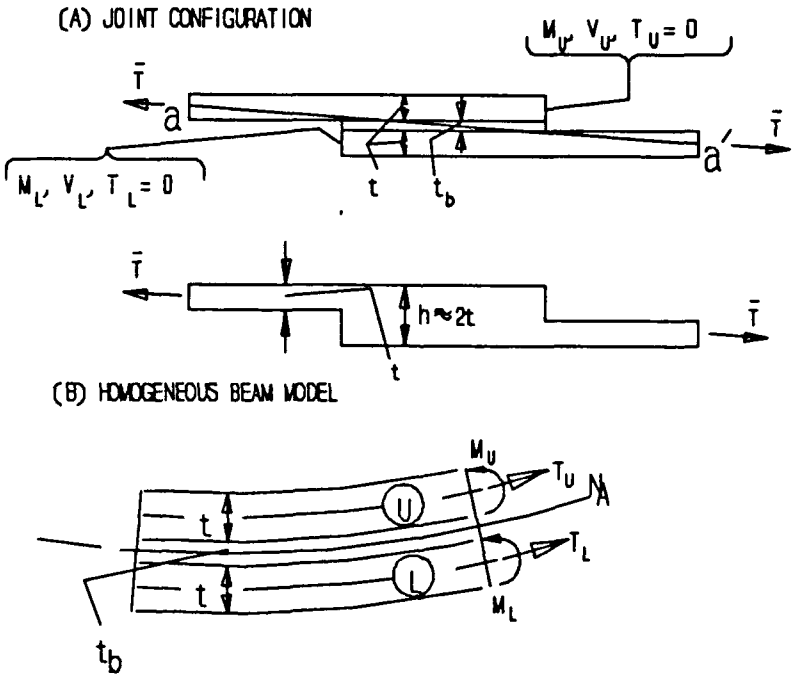

Figure 1 **Assumed Model**

A question arises with the GR analysis in the manner in which the moment is represented in the center section. The crux of the matter is the comparison of the classical moment-curvature relation for a homogeneous beam and the corresponding expression for a layered beam (i.e. Equation (1) vs. (2)):

MOMENT-CURVATURE RELATIONSHIPS

$$\textit{HomogeneousBeam:}\quad M_N = \frac{Eh^3}{12}\frac{d^2w}{dx^2} \qquad (1)$$

$$\textit{Layered Beam}\quad : \quad M_N = M_U + M_L + \frac{t}{2}(T_L - T_U) \qquad (2)$$

In the above equations, M_N represents the moment about the neutral axis, w is lateral deflection and h is the height of the homogeneous beam -- ie. approximately twice the adherend thickness, t, for a thin bond layer. With z as the thickness-wise coordinate having its origin at the mid plane of the bond layer, the remaining quantities in (1) and (2) are given by

$$M_N = -\int_{-h/2}^{h/2} z\sigma_x dz$$

$$M_U = \int_0^{h/2}(\, h/4 - z)\sigma_x dz \quad , \qquad M_L = -\int_{h/2}^{0}(z + h/4)\sigma_x dz \qquad (3)$$

$$T_U = \int_0^{h/2}\sigma_x dz \quad , \qquad T_L = \int_{-h/2}^{0}\sigma_x dz$$

Equation (1) is the classical moment-curvature relation for a homogeneous beam of height h which ignores transverse shear and thickness-wise deformations. Equation (2), on the other hand, is a statement of equilibrium of the components indicated at the right end of the segment in Figure 1(C) which make up M_N. Equation (1) happens to be equivalent to (2) under certain conditions, but these do not apply to the ends of the overlap where significant shear straining of the bond layer takes place. Because it provides for equilibrium, (2) is a mandatory relationship which it is desirable to preserve in the formulation.

It is of interest to compare (1) and (2) for the case of a homogeneous beam. Noting the standard expression for axial stress in the overlap region under combined bending and stretching (i.e. a linear function of distance from the neutral axis):

$$\sigma_x = \frac{\bar{T}}{2t} - \frac{M_N z}{I} \qquad (\textit{where } \bar{T} = T_L + T_U \;;\; I = h^3/12) \qquad (4)$$

then making use of (1) to represent M_N in (4) and introducing the latter into (3) leads to

$$M_U \equiv M_L \equiv E\frac{t^3}{12}w'' = \frac{1}{8}M_N \quad (5.1) \qquad \frac{t}{2}T_L = \frac{t}{2}\bar{T} + \frac{3}{8}M_N \quad (5.2) \qquad \frac{t}{2}T_U = \frac{t}{2}\bar{T} - \frac{3}{8}M_N \quad (5.3)$$

Since t≈h/2, Eq(5) lead to

$$M_U + M_L + \frac{t}{2}(T_L - T_U) = \frac{2}{3}Et^3\frac{d^2w}{dx^2} \equiv \frac{1}{12}Eh^3\frac{d^2w}{dx^2} \qquad (6)$$

agreeing with (2) on inserting (1) into the latter. This implies that Eq(5) have to hold in order for (1) to be applicable. In the single lap joint, however, as noted in Fig 1(A), M_L and T_L are zero at the left end of the overlap, while M_U and T_U are zero at the right end. Furthermore, in the GR analysis, M_U was represented at the left end of the overlap where (see Figure 2) $x=\ell_o$ in terms of $\bar{T}t/2$ through a dimensionless parameter k:

$$M_U(x=\ell_0) = \frac{kt}{2}\bar{T} \qquad (7)$$

where k was a function of load in the range $0.26<k<1$. Table 1 gives a comparison of required traction conditions at $x=\ell_o$ with the values for these conditions which are implied by (5) when (7) is taken into account. It is apparent that if k is not equal to unity, the required end conditions on M_L, T_U and T_L cannot be realized if (5) apply. Moreover, the fact that M_N is negative at $x=\ell_o$ while M_U is positive implies the presence of a curvature discontinuity in the upper adherend if (1) applies. **Thus Equation (1) cannot,** strictly speaking, **be used to represent M_N over the length of the overlap**. Hart Smith first pointed this out qualitatively in [3], concurring with the observation that the use of (1) requires the presence of nonzero tractions over the left end of the lower adherend. Rather than attempting to retain (1), it is desirable to use a formulation which is consistent with (2) regardless of whether or not conditions apply for which (1) is valid.

[3] HART-SMITH, L. J., *Adhesive Bonded Single Lap Joints*, NASA Contractor Report 112236 (1973)

TABLE 1. COMPARISON OF CONDITIONS FROM EQ(5) WITH TRACTIONS AT $x=\ell_o$

	REQUIRED END	VALUES IMPLIED BY
M_N	$-(1-k)\bar{T}t/2$	$-(1-k)\bar{T}t/2$
M_U	$k\bar{T}t/2$	$k\bar{T}t/2$
M_L	0	$k\bar{T}t/2$
T_U	$\bar{T}$	$(5+3k)\bar{T}/8$
T_L	0	$(11-3k)\bar{T}/8$

As suggested above, the lack of validity of Equation (1) is associated mainly with the presence of shear strains in the bond layer. More specifically, the equivalent of the following equation (see Appendix A, Eq(A-6)) which GR used to obtain the gradient of shear strain in the bond layer:

$$\frac{d\gamma}{dx} = \frac{2}{E't^2t_b}\left[\frac{t}{2}(T_U - T_L) + 3(M_U + M_L)\right]$$

gives a value of zero when (5) are allowed for, so that a condition of constant or zero shear strain in the bond is implied by (5). Lap joints typically have large shear stress and therefore strain gradients along their length due to adherend deformations, contrary to the latter result. It should be understood that the impact of shear straining on the performance of the joint is associated with the fact that organic bond materials are relatively soft compared with typical adherends. The extreme version of this situation can be visualized in terms of a beam cut along its neutral axis like a leaf spring. Since bending stiffness is a cubic function of beam depth, the bending stiffnesses of each of the two halves would be one eighth of that of the original beam. A simple analysis shows that the combined bending stiffness of the two half-beams would be the sum of the two components, amounting to 25% of that of the original beam. Thus, shear straining along the neutral axis can be expected to decrease the bending stiffness of the composite beam making up the overlap region of the joint.
In general, Equation (1) will overestimate the bending stiffness of the overlapping part of the joint, preventing correct determination of bending deflections. Since the thrust of the GR analysis was to demonstrate the influence of bending deflections on the stresses developed in the bond, an effort to correct the situation appears desirable. It should be expected that differences between predictions of the original GR approach and those of the present analysis which provides for effects bond shear straining on decoupling of the two adherends will be greater in joints containing relatively thin adherends. This is due to the fact that in the case of thicker adherends, the range of the decoupling effects is shorter and is confined to a region close to the ends of the overlap. It can be argued from St. Venant's principle that Eq(1) should be valid sufficiently far from the overlap ends, and the influence of the load diffusion process which makes it valid will be less when the effects of interest here are short in range relative to the adherend thicknesses.

In addition to the discussion of Hart Smith which was previously cited [3], problems with the GR treatment of the bending analysis have been noted by others[4-5]. Benson[4], as discussed by Adams[5], described a modification of the analysis which dealt with the situation. In addition, Hart-Smith[3] did an extensive amount of work on the single lap joint that provided an alternate method of introducing the appropriate bending deflection corrections which will be discussed subsequently.

BENSON, N. K. *Influence of Stress Distribution on Strength of Bonded Joints* in *Adhesion, Fundamentals and Practice* , Gordon and Breach, NY (1969) p. 191-205

[5] ADAMS, R.C. and WAKE, W. C. *Structural Adhesive Joints in Engineering*, Elsevier Applied Science Publishers, NY (1984)

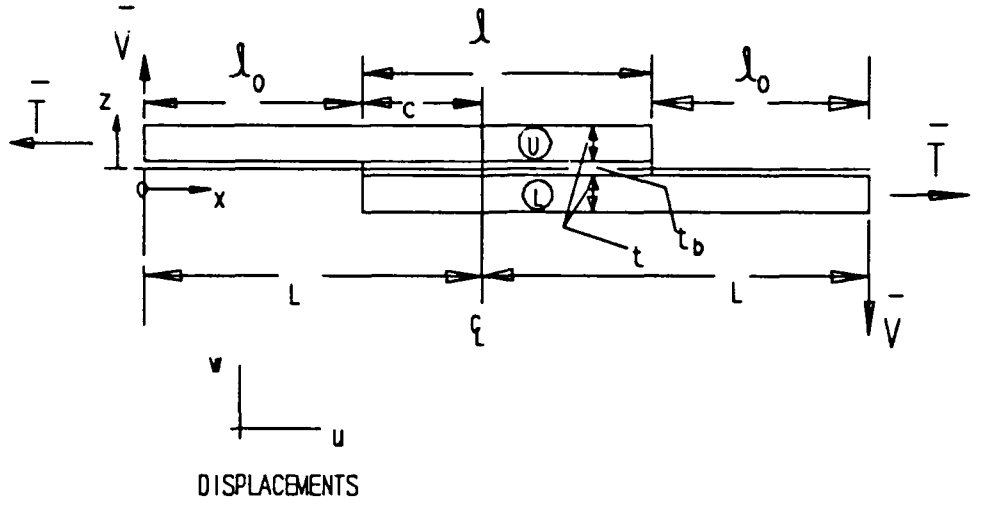

Figure 2 **Joint Geometry**

In the present case, the center section of the joint will be treated essentially as a pair of coupled beams throughout the analysis. Once again it is emphasized that GR did use the[4] coupled-beam approach to deal with of peel and shear stresses in the adhesive layer, but not in their deflection analysis.

THE ANALYSIS OF GOLAND AND REISSNER

General Remarks

It is useful here to repeat certain results which were obtained from the GR analysis. Figure

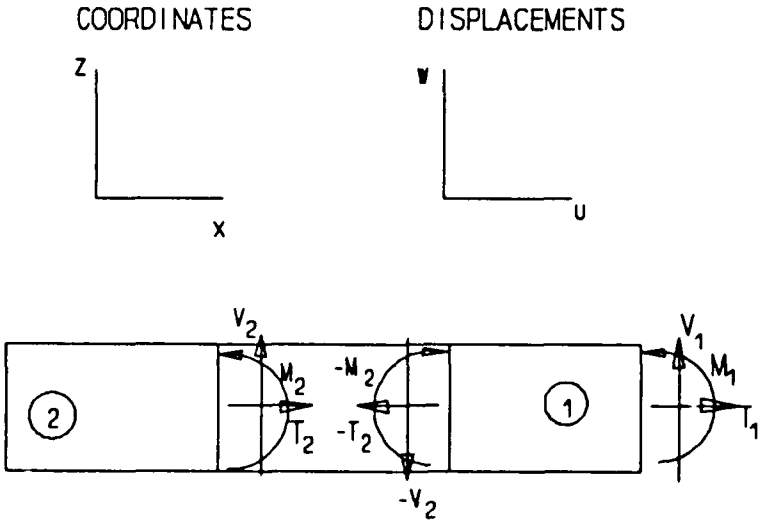

Figure 3 **Sign Conventions**

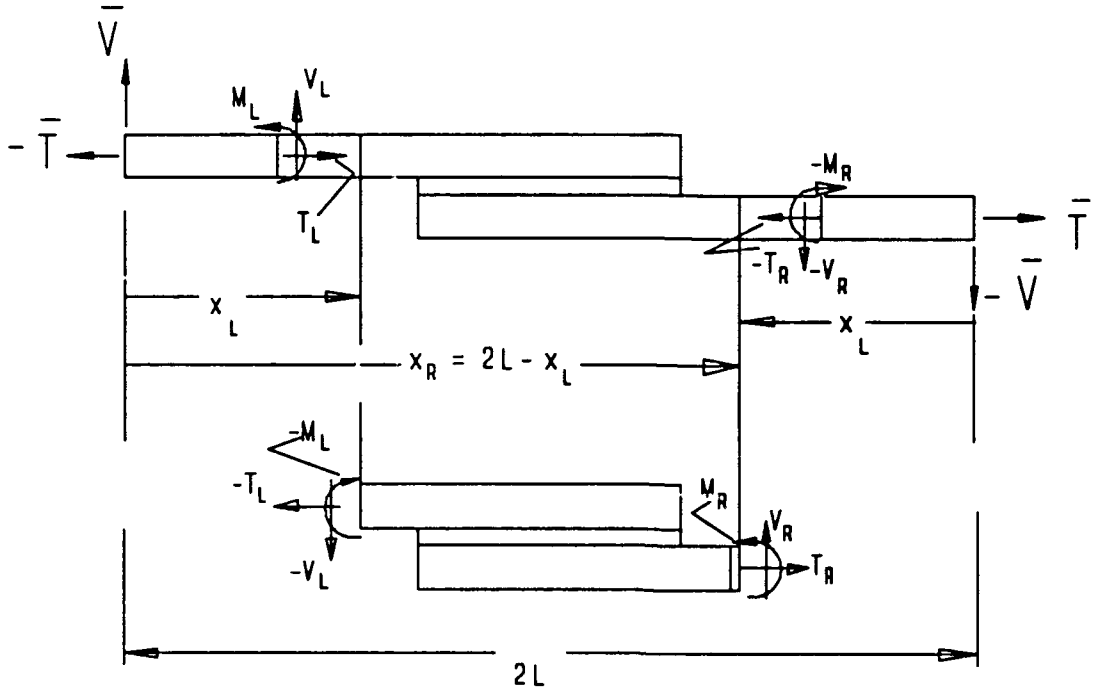

Figure 4 **Antisymmetry Conditions**

2 gives the basic parameters of interest. Here "U" and "L" denote the "upper" and "lower" adherends. The length of the adherends beyond the overlap is ℓ_o while the overlap has a length ℓ (≡2c, in the GR notation). It is assumed that tension loads (i.e. resultants) $\bar{T}$ are present at the outer ends. In terms of $\bar{T}$ it is convenient to define nominal axial stress, $\bar{\sigma}_x$, and strain, $\bar{\varepsilon}_X$:

$$\bar{\sigma}_x = \frac{\bar{T}}{t} \quad (9.1) \quad ; \quad \bar{\varepsilon}_x = \frac{\bar{\sigma}_x}{E'} \quad (9.2) \quad ; \quad E' = E/(1-\nu^2) \quad (9.3)$$

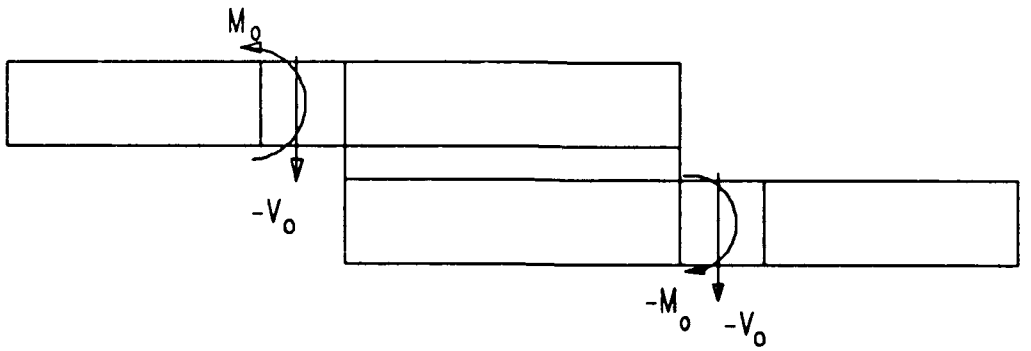

Figure 5 **End Conditions in Overlap Region**

(E, ν = Young's modulus, Poisson ratio for axial straining.) Along with $\bar{T}$, there are assumed to be transverse shear forces $\bar{V}$ which produce moment free conditions at the end points, provided

$$\bar{V} = \alpha \bar{T} \quad ; \quad \alpha = t/2L \quad ; \quad L = \ell_o + \ell/2 \equiv \ell_o + c \tag{10}$$

As in Figure 2, the directions of the transverse forces are downward at the right end and upward at the left end for moment free conditions. Fig 3 recalls standard conventions for the signs of moments, shear forces and tensions, as well as coordinates and displacements. As usual, positive moments, shear forces and tensions correspond to those shown for the right end of segment "1", while at the left end of a given segment the forces and moments are obviously the reactions to those applying to the right end of the neighboring segment (to the left of the one under consideration). Thus in Figure 3, the reactions at the left end of Segment "1" are shown as the negatives of the quantities associated with the right end of Segment "2".

Additional relationships associated with the antisymmetry of the joint are illustrated in Figure 4, where attention is focussed on points located at x_L and $x_R \equiv 2L\text{-}x_L$, i.e. points located at the same distance from each end. Equilibrium of vertical forces requires that the shear forces at these points be equal, i.e.

$$V(x_L) = V(2L - x_L) \tag{11}$$

In addition, since the generic expression V=-dM/dx holds, the fact that the moment is a function which is zero at x=L and whose derivative is symmetric about x=L requires that the moment itself be antisymmetric, i. e.

$$M(x_L) = -M(2L - x_L) \tag{12}$$

so that as shown in Figure 5, the shear forces at the ends of the overlap are equal while the moments are equal but opposite in sign. In the specific case of the ends of the overlap, GR uses the notation M_o and V_o for the moment and shear force, as indicated in Figure 5. In addition, GR expresses M_o in terms of the parameter k introduced in (7) and V_o in terms of an additional dimensionless parameter k′:

$$M_o = k\frac{t}{2}\bar{T} \quad ; \quad V_o = 2k'\bar{T}/\lambda \tag{13}$$

$$where \quad \lambda = \ell/t$$

For future reference, the end conditions on the individual adherends may be stated as in Table 2. The last four rows of Table 2 are used in forming end conditions for differential equations given in Appendix A.

Detailed Relationships

The equations encountered in the GR analysis are reviewed in Appendix A. Note that these exhibit the influence of lateral deflection on the moment distribution due to the shift in the lever arm, illustrated in Figure 6. Here the horizontal component of end load,

TABLE 2 CONDITIONS ON ADHERENDS AT ENDS OF OVERLAP		
	$x=\ell_o$	$x=\ell_o+\ell$
V_U	$-V_o \equiv -2k'\bar{T}/\lambda$	0
M_U	$M_o \equiv kt\bar{T}/2$	0
T_U	$\bar{T}$	0
V_L	0	$-V_o \equiv -2k'\bar{T}/\lambda$
M_L	0	$-M_o \equiv kt\bar{T}/2$
T_L	0	$\bar{T}$
$M_U + M_L$	M_o	$-M_o$
$T_L - T_U$	$-\bar{T}$	$\bar{T}$
$M_U - M_L$	M_o	M_o
$V_U - V_L$	$-V_o$	V_o

$\bar{T}$, acts through a load line which shifts with respect to the neutral axis of the adherend segments, as illustrated in Figure 6(A) for the outer adherend and Figure 6(B) and (C) for the overlapping part of the joint.For subsequent reference it is useful to recall the most crucial results given for the GR analysis in Appendix A at this point . These include the expressions for the quantity k:

Expressions for k

$$k = \frac{T_{h1}}{T_{h1} + \sqrt{(8)}\,T_{h2}} \quad (RPT\,A\text{-}7.6) \qquad ; \qquad k' = \frac{1}{4T_{h1}} k\lambda U \quad (RPT\,A\text{-}7.7)$$

where $T_{h1} = \tanh(U\lambda_o)$ $(RPT\,A\text{-}7.8)$; $T_{h2} = \tanh(U\lambda/2\sqrt{8})$ $(RPT\,A\text{-}7.9)$

For $T_{h1} \approx 1$

$$k = \frac{1}{1 + \sqrt{8}\,T_{h2}} \qquad ; \qquad k' = \frac{1}{4} k\lambda U \quad (RPT\,A\text{-}8)$$

together with those for the shear and peel stress solutions:

Expression for Shear Stress

$$\tau_b = -\bar{\sigma}_x[\sqrt{2}\beta\frac{(1+3k)}{4}\frac{\cosh[\sqrt{8}\beta(x-L)/t]}{\sinh\sqrt{8}\beta\lambda}+\frac{3}{4\lambda}(1-k)] \qquad (RPT\,A-10.1)$$

Maximum Value of τ_b $(x=L\pm\ell/2 \;;\; \sqrt{8}\beta\lambda/2>1 \;;\; 0.262<k<1)$

$$0.631\beta \;<\; abs\{\frac{\tau_b)_{max}}{\bar{\sigma}_x}\} \approx \sqrt{2}\beta\frac{(1+3k)}{4} \;<\; 1.414\beta \qquad (RPT\,A-10.2)$$

Maximum Value of Peel Stress $(x = L\pm\ell/2 \;;\; \gamma\lambda/2>1)$

$$\sigma_b)_{max} \approx \bar{\sigma}_x\frac{k\gamma}{2}(\gamma+U) \qquad (RPT\,A-15.3)$$

or, since $U<\gamma$ ***in practical cases:***

$$\sigma_b)_{max} \approx \bar{\sigma}_x\frac{k\gamma^2}{2}$$

Note that from the expressions given in (A-6.3) and (A-7.2) with (A-1.5), the following relation between the maximum peel and shear stress can be stated:

$$\frac{\sigma_b)_{max}}{\tau_b)_{max}} \approx \sqrt{12}\,\frac{k}{1+3k}\sqrt{\frac{E_b}{G_b}} \qquad (14)$$

If E_b/G_b is set equal to the expression for isotropic materials of $2(1+\nu_b)$ where ν_b is the Poisson ratio for the bond material, the max peel-to-shear stress ratio runs from about 2 for the upper limit of k of unity, to a little less than 1 for the lower limit ($k\approx0.26$), for an assumed Poisson ratio of around 0.5. The specific value of the assumed Poisson ratio is not important, but this estimate emphasizes that two maximum stresses take on values which are proportional to each other for various joint geometries and for which the proportionality constant is in the range of 1 to 2.

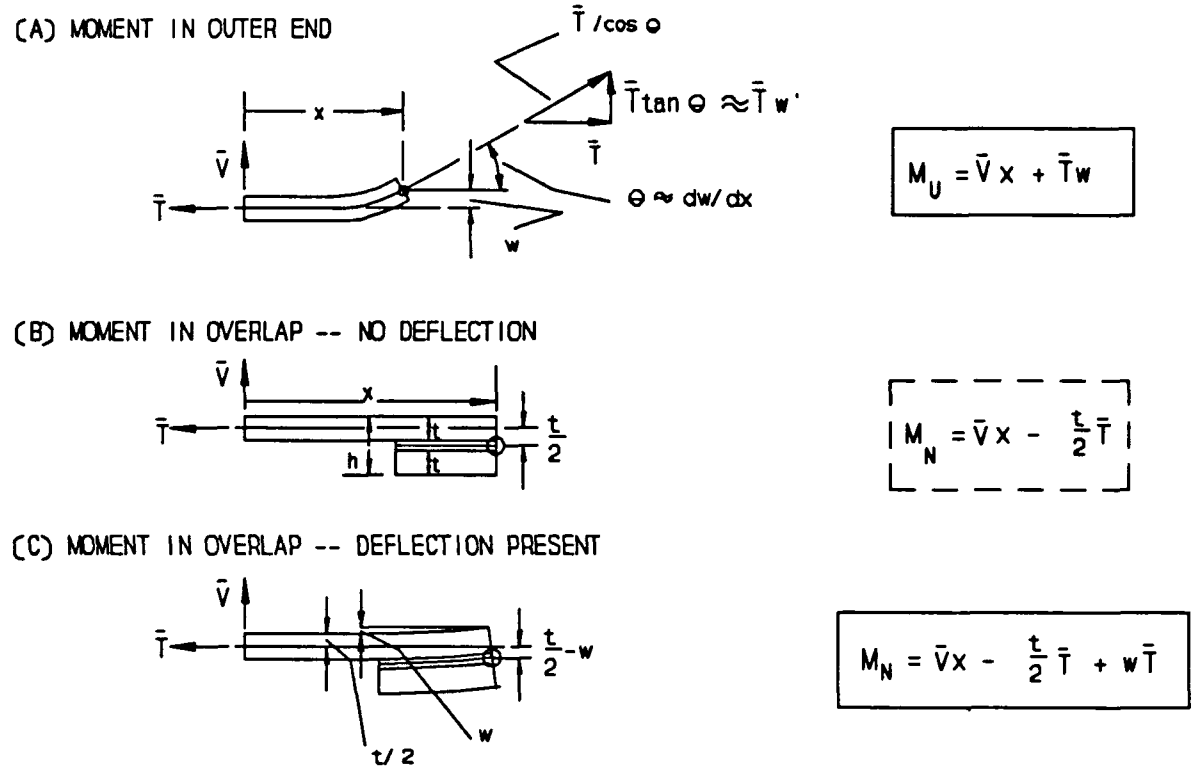

Figure 6 **Effect of Deflection on Moment Distribution**

A certain amount of controversy has arisen over the results given in Appendix A for the peel stresses (Eq(A-15)) from which (A-15.3) is obtained. Kuenzi and Stevens[6] stated a version of Eq(A-15) (coefficients of the peel stress equation) with the signs of some terms reversed from those of the GR version (see discussion following Eq(A-15)) without commenting on the justification for differing from GR. Moreover, Ref[3-4,7] claimed to have verified the version given in [6], while Carpenter[8] found the original version as given above to be valid.

Considerable care has been taken here to identify correct boundary conditions at the ends of the overlap in order to be sure that the correct expressions for peel stress coefficients were obtained. As far as can be determined, the original expressions given by GR are the correct ones. In any event, the terms in question which correspond to the term U in the second factor of (A-15.3) summarized above do not usually contribute strongly to the peel stress predictions.

[6] KUENZI, E. and STEVENS, G., *Determination of Mechanical Properties of Adhesives for Use in the Design of Bonded Joints*, Forest Products Laboratory Note FPL-011 (1963)
[7] KUTSCHA, D. and HOFER, K., *Feasibility of Joining Advanced Composite Flight Vehicle Structures*, Air Force Materials Laboratory Report AFML-TR-68-391, (1968) p. 56,59
[8] CARPENTER, W. *Goland and Reissner were Correct*, J. Strain Analysis, v. 24, no. 3 (1989)

IMPROVED ANALYSIS

Deformations and Shear Stresses

In the following discussion, it will be convenient to represent the individual adherend displacements and stress resultants in terms of differences and sums, since the bond layer stresses are more easily represented by differences in the adherend displacements and resultants than in terms of their individual values. Accordingly, the following notation is introduced:

$$\delta_T(x) = T_U - T_L \quad (15.1) \qquad \bar{w}(x) = \frac{1}{2}((w_U + w_L) \quad (15.2)$$

$$\delta_w = w_U - w_L \qquad (15.3)$$

Note that the individual adherend resultants can be expressed in terms of $\bar{T}$ and $\delta_T(x)$, as follows:

$$T_U = \frac{1}{2}[\bar{T} + \delta_T(x)] \quad ; \quad T_L = \frac{1}{2}[\bar{T} - \delta_T(x)] \qquad (16)$$

In addition, note that the quantity M_U+M_L, which appears in Eq(2) as well as (A-6.1) for the assumed case of identical adherends, is given by

$$M_U + M_L = 2D_U\frac{d^2\bar{w}}{dx^2} \quad (17)$$

For increased accuracy in the following, the quantity t/2 appearing in Eq(2) and (A-2.2) will be replaced by $(t+t_b)/2$ to provide for the effect of bond layer thickness. The replacement of Eq(1) by (2) modified in this way can then be accommodated by using Eq(A-1.3, .4) to represent M_U and M_L in terms of displacements (setting $D_U=D_L$) i.e.:

$$M_N = D_U(\frac{d^2w_U}{dx^2} + \frac{d^2w_L}{dx^2}) - \frac{t+t_b}{2}(T_U - T_L)$$

or, in terms of the notation just introduced,

$$M_N = D_U\frac{d^2\bar{w}}{dx^2} - \frac{t+t_b}{2}\delta_T \quad . \qquad (18)$$

Then equating the modified form of (A-2.2) with (18) (letting the neutral axis displacement be represented by $\bar{w}$) leads to

$$D_U\frac{d\bar{w}^2}{dx^2} - \frac{t+t_b}{2}\delta_T = \bar{T}\alpha x - (\frac{t+t_b}{2} - \bar{w})\bar{T} \qquad (19)$$

Note that, as opposed to the original GR analysis, coupling occurs between $\bar{w}$ and the adherend resultants, so that $\bar{w}$ cannot be determined independently of δ_T in the updated analysis. A second

equation in $\bar{w}$ and δ_T is obtained by multiplying (A-6.1) by G_b to get $d\tau_b/dx$ on the left which, according to (A-3.1), is equivalent to d^2T_U/dx^2, or equivalently (according to the left member of (16)) to $(d^2\delta_T/dx^2)/2$. Then again allowing for the assumption of identical adherends, making use of (15.1) and (17) leads to

$$\frac{d^2\delta_T}{dx^2} = \frac{2G_b}{t_b}\left(\frac{1}{B_U}\delta_T + t\frac{d^2\bar{w}}{dx^2}\right) \qquad (20)$$

We can combine Eq(19) and (20) with (A-5.1) (which there was no need to modify) and obtain a self-contained system of differential equations for $\bar{w}$ and δ_T. After transposing and re-applying previously developed notation, we get

Displacement in Outer Segment of Adherend $(x \le \ell_o)$

$$\frac{d^2w_U}{dx^2} - \frac{U^2}{t^2}w_U = \frac{U^2}{t^2}\alpha x \qquad (21.1)$$

Displacement in Overlapping Segment of Joint $(x \le \ell_o \le \ell_o + \ell)$

$$\frac{d^2\bar{w}}{dx^2} - \frac{U^2}{8t^2}\bar{w} = \frac{U^2}{8t^2}\left(\alpha x - \frac{t+t_b}{2}\right) + \frac{t+t_b}{2}\frac{1}{D_U}\delta_T \qquad (21.2)$$

ResultantDifference $(x \le \ell_o \le \ell_o + \ell)$

$$\frac{d^2\delta_T}{dx^2} - 2\frac{\beta^2}{t^2}\delta_T = 2G_b\frac{t}{t_b}\frac{d^2w}{dx^2} \qquad (21.3)$$

Eq(21.2, .3) can be solved as a 2x2 system. Boundary conditions include the end conditions on δ_T in terms of the values of T_U and T_L given in Table 2, together with the joining conditions on the displacements at $x=\ell_o$. The homogeneous part of this system can be written

$$\bar{w}_h'' - \frac{U^2}{2t^2}\bar{w}_h - \frac{t+t_b}{2}\delta_{Th} = 0 \qquad (22.1)$$

$$\delta_{Th}'' - 2\frac{\beta^2}{t^2}\delta_{Th} - 2\beta^2 E'\bar{w}_h'' = 0 \qquad (22.2)$$

where U and β which are key parameters in the GR analysis (EQ(A-8, A-9) are defined by

$$U = t\sqrt{\bar{T}/D_U} \equiv \sqrt{12\bar{\varepsilon}_x} \quad ; \quad \beta = \sqrt{\rho_G/\rho_t} \quad \textit{where} \quad \rho_g = G_b/E' \; ; \; \rho_t = t_b/t$$

These represent exponential decay factors in the functions describing bending and bond shear stress distribution along the overlap region in the GR analysis. Solutions to (22) can be expressed as exponential functions:

When substituted into (22), these lead to a 2x2 system of algebraic equations with Δ_h,

$$\bar{w}_h = W_h e^{\mu x/t} \quad ; \quad \delta_{Th} = \Delta_h e^{\mu x/t} \qquad (23)$$

W_H and μ as unknowns:

$$(2\mu^2 - U^2)E'W_h - 6(1+\rho_t)\Delta_h = 0 \qquad (24.1)$$

$$-2\beta^2\mu^2 E'W_h + (\mu^2 - 2\beta^2)\Delta_h = 0 \qquad (24.2)$$

The following notation in terms of U and β, will be useful:

$$R = U/\beta \quad (25.1) \qquad \nu_j (j=1,2) = \mu_j^2/\beta^2 \quad (25.2)$$

$$R_1 = \sqrt{8}\,\mu_1/U \quad (25.3) \qquad R_2 = \mu_2/\{\sqrt{85}\,\beta\} \quad (25.4)$$

where μ_j are the roots of the polynomial

$$\mu^4 - [(8 + \frac{6}{\rho_t}) + \frac{R^2}{2}]\beta^2\mu^2 + R^2\beta^4 = 0 \quad (26)$$

obtained from setting the determinant of (24.1, .2) *to zero.*

Note that we can express R given in (25.1), in terms of U and β, as

$$R \equiv \sqrt{12\frac{\bar{\sigma}_x}{G_b}\frac{t_b}{t}} \qquad (27)$$

from which we observe that as the adherend thickness, t, grows, R approaches zero. In addition, Eq(25) give us, for R_1 and R_2

$$\mu_1 = \frac{R_1}{\sqrt{8}} R\beta \quad (28.1) \quad ; \quad \mu_2 = \sqrt{8}\,R_2\beta \quad (28.2)$$

which, taking note of (25.2), *leads to*

$$R_1 = \frac{\sqrt{8\nu_1}}{R} \quad (28.3) \quad ; \quad R_2 = \sqrt{\frac{\nu_2}{8}} \quad (28.4)$$

In terms of ν (suppressing the j subscript), Eq(26) can be expressed as

$$\nu^2 - [8(1 + \frac{3}{4\rho_t}) + \frac{R^2}{2}]\nu + R^2 = 0 \quad (29)$$

The roots of (29) are of the form

$$\nu_1, \nu_2 = a \pm b \quad (30.1) \qquad \textit{where} \qquad a = [4(1 + \frac{3}{4}\rho_t) + \frac{R^2}{4}] \quad (30.2) \quad ; \quad b = \sqrt{a^2 - R^2} \quad (30.3)$$

It is useful to observe here that the standard identity between the constant term of a quadratic expression and the product of its roots, when applied to (29), implies that $\nu_2 \equiv R^2/\nu_1$. When this relationship is applied to (28.3, .4), the following relationship:

$$R_2 \equiv \frac{1}{R_1} \qquad (31)$$

is obtained. For most practical situations, the value of R obtained from (27) will be on the order of 1 or less. On the other hand, the quantity "a" given in (30.2) can not be less than 4, so that in general we have $R^2 << a^2$. Accordingly, a binomial expansion of (30.3) gives the approximation

$$b \approx a - \frac{R}{2a} \qquad (32)$$

from which (30) lead to

$$\nu_1 \approx \frac{R}{2a} \quad (33.1) \qquad ; \qquad \nu_2 \approx 2a \quad (33.2)$$

or, making use of (28.3, .4) followed by (28.1, .2):

$$R_1 \approx \frac{2}{\sqrt{a}} \quad (34.1) \qquad ; \qquad R_2 \approx \frac{\sqrt{a}}{2} \quad (34.2)$$

i.e. for large t, for which $(\rho_t, R) \rightarrow 0$ *and* $a \rightarrow 4$:

$$R_1 \approx R_2 \approx 1 \qquad (34.3)$$

$$\mu_1 \approx R\frac{\beta}{\sqrt{8}} \equiv \frac{U}{\sqrt{8}} \quad ; \quad \mu_2 \approx \sqrt{8}\,\beta \qquad (35)$$

which are the roots of the differential equations in the original GR analysis for deflection of the center part of the joint and the bond shear stresses. In the updated analysis, the solution given in (A-7.1) for the outer part of the adherend is still applicable, while for the overlapping part of the joint, the complete solution corresponding to Eq(21.2, .3) is a combination of the exponential functions appearing in (23) containing the coefficients $\pm\mu_1$ and $\pm\mu_2$ (arranged terms of hyperbolic functions to accommodate the anti-symmetry of the problem) plus a linear term representing the particular solution of (21.2). In the following it is convenient to express the coefficients of terms describing $\bar{w}$ as multiples of t/2, as was done earlier. Thus the coefficients

W_{hj} (j=1,2), where j corresponds to which root of (26) is referenced, can be conveniently expressed in terms of t/2 by

$$W_{hj}(j=1,2) = k_{2j}\frac{t}{2} \qquad (36)$$

The complete solution for $\bar{w}$ and δ_T is then given by

$\ell_o < x < \ell_o + \ell$

$$\bar{w} = \frac{t}{2}k_{21}\frac{\sinh[\mu_1(x-L)/t]}{\sinh(\mu_1\lambda/2)} + \frac{t}{2}k_{22}\frac{\sinh[\mu_2(x-L)/t]}{\sinh(\mu_2\lambda/2)} + \frac{t}{2} - \alpha x \qquad (37.1)$$

$$\delta_T = \Delta_{h1}\frac{\sinh[\mu_1(x-L)/t]}{\sinh(\mu_1\lambda/2)} + \Delta_{h2}\frac{\sinh[\mu_2(x-L)/t]}{\sinh(\mu_2\lambda/2)} \qquad (37.2)$$

It is convenient to express the coefficients of Eq(37.2) as well as (37.1) in terms of k_{2j}. For this purpose note that (24.2) together with (36) imply that Δ_{hj} and k_{2j} are related by

$$\Delta_{hj}(j=1,2) = H_j E' k_{2j}\frac{t}{2} \qquad (38.1) \qquad \textit{where} \qquad H_j = \frac{2\beta^2\mu_j^2}{\mu_j^2 - 2\beta^2} \qquad (38.2)$$

From Eq(9) together with the definition of U following (22), we can substitute

$$E't = 12\frac{\bar{T}}{U^2}$$

into (38.1) to eliminate E't. In addition, it is useful to express the H_j's in terms of the roots $U/(8)^{1/2}$ and $(8)^{1/2}\beta$ of the GR deflection and bond shear stress analysis, as follows:

$$H_1 = -J_1\left(\frac{U^2}{8}\right) \equiv -J_1\frac{(R\beta)^2}{8} \qquad (39.1) \qquad ; \qquad H_2 = J_2(8\beta^2) \qquad (39.2)$$

where the J_j's are constants to be determined. Substituting (39) into (38.1) together with the expression for E't just given then leads to

$$\Delta_{h1} = \frac{3}{4}J_1 k_{21}\bar{T} \qquad (40.1) \qquad ; \qquad \Delta_{h2} = 48J_2\frac{k_{22}}{R^2}\bar{T} \qquad (40.2)$$

In addition, substitution of (38.2) into (39), representing the μ_j's in terms of (28.1, .2), and allowing for (31), leads to

$$J_1 = \frac{1}{R_2^2 - \frac{R^2}{16}} \qquad (41.1) \qquad ; \qquad J_2 = \frac{R_2^2}{4R_2^2 - 1} \qquad (41.2)$$

In the following, the deflection equation, (A-7.1), for $x< \ell_o$, will be expressed in terms of revised notation in which "k_n" (the subscript "n" designating "new") will be substituted for the "k" of the original GR analysis, ie. (A-7.1) is expressed as

$x<\ell_o$

$$w = \frac{t}{2} k_n \frac{\sinh(Ux/t)}{\sinh(U\lambda_o)} - \alpha x \qquad (42)$$

Continuity conditions at $x=\ell_o$ can now be established to obtain equations for determining k_n together with the k_{2j}'s. Note here that for practical purposes, the displacements of the neutral axis in the region of overlap may be taken as equivalent to that of either adherend, since the actual difference is on the order of the adhesive peel strain times the adhesive layer thickness, a much smaller quantity than w_U, w_L or $\bar{w}$ can be expected to amount to. Thus the displacement of the outer adherend can be considered equal to that of the neutral axis at $x=\ell_o$ and similarly with the slopes. Continuity requirements then amount to equating the value and derivative of $\bar{w}$ given by (37.1) with those of w given by (42) for $x=\ell_o$ [i.e. $(x-L)/t = -\lambda/2$] as well as setting δ_T given by (37.2) to $\bar{T}$ at that location. After canceling out common factors of $\bar{T}$ and t/2, three equations relating k_n, k_{21} and k_{22} are obtained:

$$-\frac{3}{4} J_1 k_{21} + 48 \frac{J_2}{R^2} k_{22} = -1 \qquad (43.1)$$

$$k_{21} + k_{22} + k_n = 1 \qquad (43.2)$$

$$R_1 R k_{21} + 8 R_2 \frac{T_{h21}}{T_{h22}} k_{22} - \sqrt{8} R \frac{T_{h21}}{T_{h1}} k_n = 0 \qquad (43.3)$$

$$\textit{where } T_{h2j} = \tanh(\mu_j \lambda/2) \qquad (43.4)$$

A straightforward elimination approach can be used, here in which (43.1) is first transposed to get k_{22} in terms of k_{21}:

$$k_{22} = R^2 (C_1 k_{21} - C_2) \qquad (44.1)$$

where

$$C_1 = \frac{K_1}{K_2} \quad ; \quad C_2 = \frac{1}{K_2} \quad ; \quad K_1 = \frac{3}{4} J_1 \quad ; \quad K_2 = 48 J_2 \qquad (44.2)$$

which may be substituted into (43.2) to eliminate k_{22}:

$$(1+R^2C_1)k_{21} - R^2C_2 + k_n = 1$$

or, after transposing:

$$k_{21} = \frac{1+R^2C_2-k_n}{1+R^2C_1} \qquad (45)$$

Back-substituting this into (44.1) to eliminate k_{21} gives

$$k_{22} = R^2(C_1\frac{1+R^2C_2-k_n}{1+R^2C_1} - C_2) \qquad (46)$$

Finally, substituting (45) and (46) into (43.3) provides an expression for k_n of the form

$$R_1R\frac{1+R^2C_2-k_n}{1+R^2C_1} + 8R_2\frac{T_{h21}}{T_{h22}}\frac{R^2(C_1-C_2)-R^2C_1k_n}{1+R^2C_1} - \sqrt{8}\frac{T_{h21}}{T_{h22}}k_n = 0$$

which transposes to give:

$$k_n = \frac{R_1(1+R^2C_2) + 8R_2\frac{T_{h21}}{T_{h22}}R(C_1-C_2)}{R_1 + 8R_2\frac{T_{h21}}{T_{h22}}RC_1 + \sqrt{8}(1+R^2C_1)\frac{T_{h21}}{T_{h1}}} \qquad (47)$$

As noted previously [Eq(27)], R tends toward zero for large t, so that all the terms in (47) containing R as a factor will disappear, while R_1 and R_2 approach unity. We then have:

$t>>t_b$ $(R,\rho_t\to 0)$

$$k_n \to \frac{1}{1+\sqrt{8}\dfrac{T_{h21}}{T_{h1}}} \qquad (48)$$

i.e. k_n approaches the value given in the GR analysis for their "k" given by (A-7.6). (It can easily be shown that T_{h21} of the present analysis approaches T_{h2} of the GR analysis.) In addition, substituting (30.2) into (49.2) and the latter into (54) gives

$t>>t_b$ $(R,\rho_t\to 0)$

$$J_1 \approx \frac{1}{1+\frac{3}{4}\rho_t} \quad ; \quad J_2 \approx \frac{1}{3}\frac{1+\frac{3}{4}(\rho_t+\frac{1}{12}R^2)}{1+(\rho_t+\frac{1}{12}R^2)} \qquad (49)$$

From (49) it is apparent that we can set

$$J_1 \approx 1,\ J_2 \approx 1/3 \quad (t>>t_b), \qquad (50)$$

and making use of the notation of (44.2) as well as (45, 46) leads to

$t>>t_b$ $(R,\rho_t\to 0)$

$$k_{21} \approx 1-k_n \quad ; \quad k_{22} \approx \frac{R^2}{16}[\frac{3}{4}(1-k_n)-1] \approx 0 \qquad (51)$$

which is again consistent with GR. Applying (50, (51)) to (41) then leads to

$t>>t_b$ $(R,\rho_t\to 0)$

$$\Delta_{h1} \approx -\frac{3}{4}(1-k_n)\bar{\sigma}_x t \quad ; \quad \Delta_{h2} \approx [\frac{3}{4}(1-k_n)-1]\bar{\sigma}_x t \qquad (51)$$

At this point we focus attention on the bond layer shear stress distribution. Noting the relation between T_U and δ_T given in (15) and applying (A-3.1) to (36.2) with T_U expressed in terms of δ_T leads to the following for τ_b:

$$\tau_b = \frac{\mu_1}{2t}\Delta_{h1}\frac{\cosh[\mu_1(x-L)/t]}{\sinh(\mu_1\lambda/2)} + \frac{\mu_2}{2t}\Delta_{h2}\frac{\cosh[\mu_2(x-L)/t]}{\sinh(\mu_2\lambda/2)} \qquad (52)$$

For the case of $t>>t_b$, substituting (51) into (52) and allowing for (49) results in

$t>>t_b$ $(R,\rho_t\to 0)$

$$\tau_b \approx \sigma_b[\frac{\sqrt{8}\,\beta}{8}(1+3k_n)\frac{\cosh[\sqrt{8}\,\beta(x-L)/t]}{\sinh(\sqrt{8}\,\beta\lambda/2)} + \frac{3}{8\sqrt{8}}U(1-k_n)\frac{\cosh[U(x-L)/\sqrt{8}\,t]}{\sinh(u\lambda/2\sqrt{8})}] \qquad (53)$$

from which the maximum value of shear stress in the bond layer is approximately

$t>>t_b$ $(R,\rho_t\to 0)$

$$\frac{\tau_b)_{max}}{\bar{\sigma}_x} \approx \frac{\sqrt{8}\,\beta}{8}(1+3k_n)\frac{1}{T_{h22}} + \frac{3}{8\sqrt{8}}U(1-k_n)\frac{1}{T_{h21}} \qquad (54)$$

Note that as in the case of k_n given by (46), Eq(54) is in essential agreement with Eq(A-10) obtained by GR, except that the second term in the latter disappears for sufficiently large λ

(i.e. dimensionless overlap length), whereas here the second term persists no matter how long the joint is.

Peel Stresses in the Modified Analysis

Note that (see Eq(A-2.2), Appendix A) the same expression (Eq(2)) for M_N, the moment about the neutral axis, applies for the present analysis as that used by GR. However, for the individual adherends, this needs to be examined further to insure a correct version of the formulation for the peel stresses. In particular, the influence of bond shear and peel stresses on the moments in the individual adherends has to be re-examined. In the following, it will turn out that the influence of **peel** stresses on the adherend moment distribution will be unchanged from what it was in the GR analysis. However, the contribution of the **shear** stresses on adherend moments is influenced by adherend deflections through the same mechanism as that which applied to the moments generated by the horizontal components of the end loads. A particular point which should be understood has to do with the way that these horizontal loads generate moments at various points in the adherends. These are **not** large deflection effects corresponding to large values of either lateral deflection or slope. Rather, they should be thought of as **long range** effects, since they correspond to relatively large horizontal offsets between the point where the load is generated and the point under consideration where moments are being calculated. Figure 7(A) denotes the incremental loads, $dF_\tau(\hat{x})$ and $dF_\sigma(\hat{x})$ generated on the upper adherend by the shear and peel stresses at a generic axial position $\hat{x}$, where

$$dF_\tau(\hat{x}) = \tau_b d\hat{x} \quad ; \quad dF_\sigma(x) = \sigma_b d\hat{x}$$

As stated previously, the theory developed here is a small strain, small deflection theory. Thus, for example, rotation will produce a vertical component of dF_τ given approximately by $w'dF_\tau$ at $\hat{x}$ which will produce a moment contribution at x given by $(\hat{x}-x)w'dF_\tau$. The fact that w' is assumed to be a negligible quantity does not rule out the possibility that $(x-\hat{x})w'$ may not be if $x-\hat{x}$ is large enough.

On the other hand, a similar horizontal component of dF_σ given approximately by $w'dF_\sigma$ produces a moment at x given by $[w(x)-w(\hat{x})]w'dF_\sigma$; but since $w(x)-w(\hat{x})$ is equivalent to $(x-\hat{x})w'_{ave}$ where w'_{ave} is the average slope in the interval between $\hat{x}$ and x, the contribution of the rotation of dF_σ is of the order of $(x-\hat{x})w'^2dF_\sigma$, i.e. proportional to the square of the slope, and can be ignored in comparison with $w'(x-\hat{x})dF_\tau$. Thus, while the rotation of dF_σ can be ignored in a small-slope analysis, that of dF_τ cannot necessarily be similarly ignored. Accumulation of dF_τ and dF_σ by integration along the adhesive-adherend interface will then produce a moment at the point of observation, x, which is determined by the offset of the load lines of incremental loads dF_τ and dF_σ, applied at $\hat{x}$, from the point of observation, ie. by ℓ_σ and ℓ_τ shown in Figure 7(B). The adherend moments can thus be written as

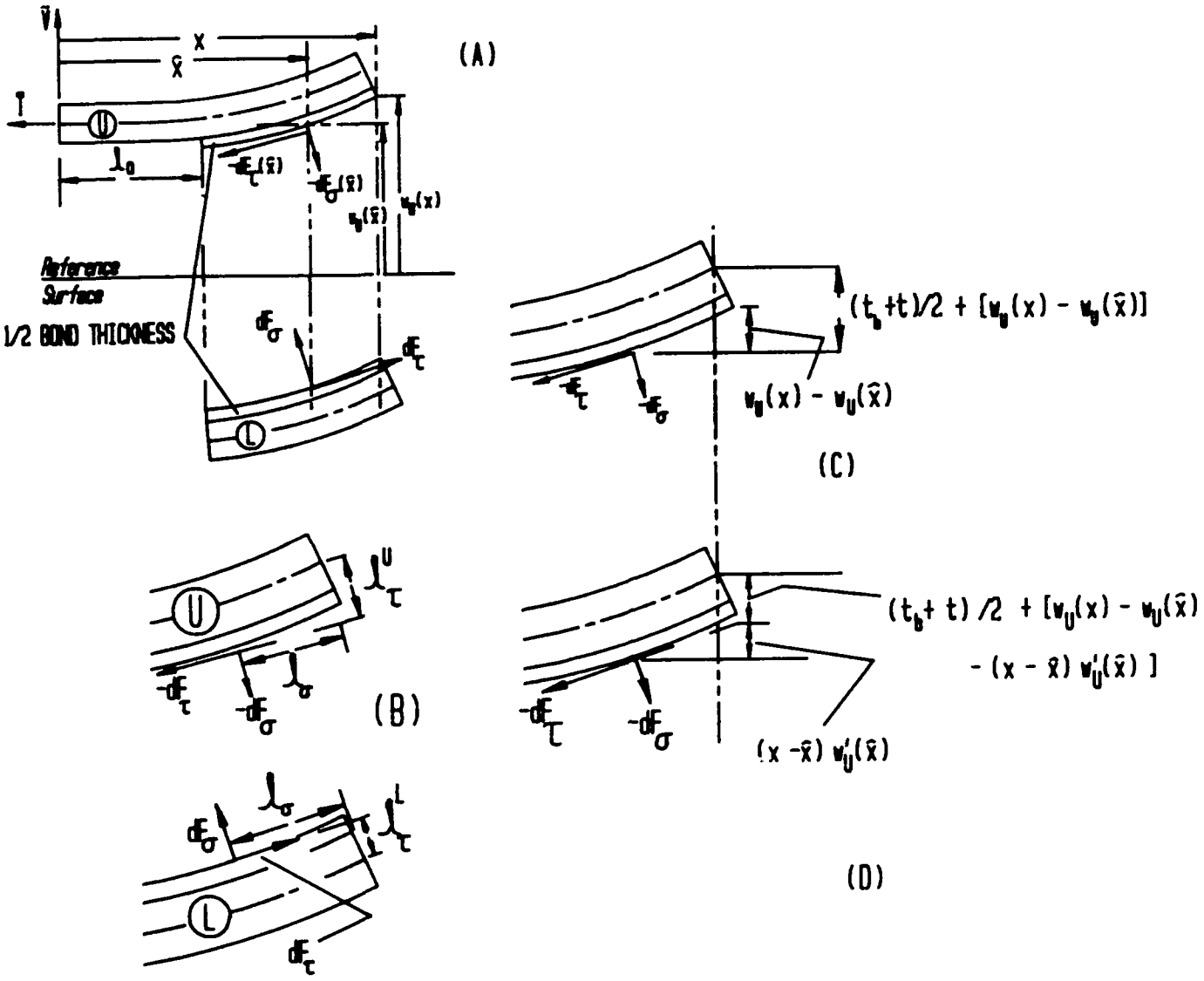

Figure 7 Effects of Adherend Deflections on Moments in Overlap Region

$$M_U(x) = \bar{V}x + \bar{T}w_U(x) + \int_{x_o}^{x} \ell_\tau^U(x,\hat{x})\,dF_\tau(\hat{x}) - \int_{x_o}^{x} \ell_\sigma(x,\hat{x})\,dF_\sigma(\hat{x}) \quad ; \quad M_L(x) = \int_{x_o}^{x} \ell_\tau^L(x,\hat{x})\,dF_\tau + \int_{x_o}^{x} \ell_\sigma(x,\hat{x})\,dF_\sigma$$

$$\textit{where} \qquad \ell_\sigma = x - \hat{x}$$

for both adherends, while expressions for ℓ_τ^U and ℓ_τ^L are obtained as follows: for the upper adherend, as illustrated in Figure 7(C) and (D), the load produced by dF_τ at $\hat{x}$ is offset from the neutral axis at x by ℓ_τ^U given by

UpperAdherend

$$\ell_\tau^U = \frac{1}{2}(t+t_b) + [w_U(x) - w_U(\hat{x}) - (x-\hat{x})w_U'(\hat{x})] \qquad (55)$$

This is obtained from considering various contributions to ℓ_τ shown in Figure 7. It is clear, first of all, that a moment is generated by dF_τ from the difference in w_U at $\hat{x}$ and x, as shown in Figure 7(C). In addition, as in Figure 7(D) (lower expression at right end of adherend segment), the tilt of the tangent vector at $\hat{x}$ has the effect of counteracting the latter displacement difference by an amount $(x-\hat{x})w'$, resulting in Eq(55)). As apparent in Figure 7(B),however, the deflection of the **lower** adherend tends to move its neutral axis **toward** the load line of dF_τ rather than away from it as in the case of the upper adherend. As a result, the terms in Eq(55) which are in square brackets are **subtracted** for the lower adherend rather than added, resulting in

$$\ell_\tau^L = \frac{1}{2}(t+t_b) - [w_L(x) - w_L(\hat{x}) - (x-\hat{x})w_L'(\hat{x})] \qquad (56)$$

inserting Eq(55) and (56) into the integral expressions just given for the moments in the adherends at a generic observation point x, ($x \geq \ell_o$) leads to:

$$M_U = \bar{V} + \bar{T}w_U(x) + \int_{\ell_o}^{x} \tau_b(\hat{x}) \{ \frac{1}{2}(t+t_b) + [w_U(x) - w_U(\hat{x}) - (x-\hat{x})w_U'(\hat{x})] \} d\hat{x} + \int_{\ell_o}^{x} (x-\hat{x})\sigma_b(\hat{x})\, d\hat{x} \qquad (57.1)$$

and

$$M_L = \int_{\ell_o}^{x} \tau_b(\hat{x}) \{ \frac{1}{2}(t+t_b) - [w_L(x) - w_L(\hat{x}) - (x-\hat{x})w_L'(\hat{x})] \} d\hat{x} - \int_{\ell_o}^{x} (x-\hat{x})\sigma_b(\hat{x})\, d\hat{x} \qquad (57.2)$$

Derivatives of Eq(57) are needed for the subsequent development. These are obtained by use of the following identities which apply to arbitrary functions F(x), G(x) and H(x):

$$\frac{d}{dx}\int_{\ell_o}^{x} H(\hat{x})\, d\hat{x} = H(x)$$

from which

$$\frac{d}{dx}\int_{\ell_o}^{x} F(\hat{x})G(\hat{x})\, d\hat{x} = F(x)G(x) \quad ; \quad \frac{d}{dx}\int_{\ell_o}^{x} F(\hat{x})G(x)\, d\hat{x} = G'(x)\int_{\ell_o}^{x} F(\hat{x})\, d\hat{x} + G(x)F(x)$$

leading to

$$\frac{d}{dx}\int_{\ell_o}^{x} [G(x) - G(\hat{x})]F(\hat{x})\, d\hat{x} = G'(x)\int_{\ell_o}^{x} F(\hat{x})\, d\hat{x} \qquad (58)$$

Applying this to (57) leads to

$$\frac{dM_U}{dx} = \bar{V} + \bar{T}w_U'(x) + \frac{1}{2}(t+t_b)\tau_b(x) - \int_{\ell_o}^{x} [w_U'(x) - w_U'(\hat{x})]\tau_b(\hat{x})\, d\hat{x} - \int_{\ell_o}^{x} \sigma_b(\hat{x})\, d\hat{x} \qquad (59.1)$$

$$\frac{dM_L}{dx} = \frac{1}{2}(t+t_b)\tau_b(x) - \int_{\ell_o}^{x} [w_L'(x) - w_L'(\hat{x})]\tau_b(\hat{x})\, d\hat{x} + \int_{\ell_o}^{x} \sigma_b(\hat{x})\, d\hat{x} \qquad (59.2)$$

while differentiating (59) to get second derivatives of M_U and M_L results in

$$\frac{d^2M_U}{dx^2} = \bar{T}w_U''(x) + \frac{1}{2}(t+t_b)\tau_b(x) + w_U''(x)\int_{x_o}^{x}\tau_b(\hat{x})d\hat{x} - \sigma_b(x) \quad (60.1)$$

$$\frac{d^2M_L}{dx^2} = \frac{1}{2}(t+t_b)\tau_b(x) - w_L''(x)\int_{x_o}^{x}\tau_b(\hat{x})d\hat{x} + \sigma_b(x) \quad (60.2)$$

Making use of (16.2, .5) and (30) to eliminate the integral expressions in (60) then leads to

$$\frac{d^2M_U}{dx^2} = T_U(x)w_U''(x) + \frac{1}{2}(t+t_b)\tau_b'(x) - \sigma_b \quad (61.1)$$

$$\frac{d^2M_L}{dx^2} = T_L(x)w_L''(x) + \frac{1}{2}(t+t_b)\tau_b'(x) + \sigma_b \quad (61.2)$$

and subtracting (61.2) from (61.1) results in

$$\frac{d^2(M_U-M_L)}{dx^2} = (T_Uw_U'' - T_Lw_L'') - 2\sigma_b \quad (62)$$

Note the identity

$$T_Uw_U'' - T_Lw_L'' = \frac{1}{2}(T_U+T_L)(w_U''-w_L'') + \frac{1}{2}(T_U-T_L)(w_U''+w_L'')$$

or, making use of (16.7) together with the notation of (30),

$$T_Uw_U'' - T_Lw_L'' = \bar{T}\delta_w'' + \delta_T\bar{w}'' \quad (63)$$

On allowing for (14.3, .4) and (17.2, .4), the second derivative of the difference between adherend moments can be expressed as :

$$\frac{d^2(M_U-M_L)}{dx^2} \equiv D_U\frac{d^4\delta_w}{dx^4} = D_Ut_b\frac{d^4\varepsilon_b}{dx^4} \equiv D_U\frac{t_b}{E_b}\frac{d^4\sigma_b}{dx^4} \quad (64)$$

while from the same relationships, the right hand side of (63) can be expressed as

$$\bar{T}\delta_w'' + \delta_T\bar{w}'' = \bar{T}\frac{t_b}{E_b}\frac{d^2\sigma_b}{dx^2} + \delta_T\bar{w}'' \quad (65)$$

Inserting (65) into (63) and the result of that substitution, together with (64), into (62) then results in

$$\frac{d^4\sigma_b}{dx^4} - \frac{U^2}{2t^2}\frac{d^2\sigma_b}{dx^2} + \frac{4\gamma^4}{t^4}\sigma_b = \frac{2\gamma^4}{t^4}\delta_T\bar{w}'' \quad (66)$$

The last equation is comparable to (20.1) obtained by GR for the peel stresses, with the addition of the second order term on the left and the forcing function on the right. The homogeneous solution for (66) will be of a form similar to (26) for the GR peel stress analysis, except for minor changes having to do with the fact that the coefficients for the

trigonometric factors in (24) will be slightly different from those for the factors involving hyperbolic functions. In practice, the changes are so small as to be of no practical significance, so that (26), with an appropriate modification of k, can be used for the homogeneous solution for all intents and purposes.

The presence of a non-zero function on the right side of (66) requires the addition of a particular solution to the homogeneous solution. Obviously, the factors from which the right hand side is formed are obtained from the solutions for $\bar{w}$ and δ_T given in (51). The details of this part of the solution will be provided in Appendix B. Again it will be found that in practical situations, the differences introduced by these terms from those of the GR peel stress expression (except for the replacement of k by k_n) are essentially negligible.

COMMENTS ON THE HART-SMITH ANALYSIS

To date, the only serious attempt to correct the deficiencies of the GR deflection analysis, other than the present one, appears to have been that of Hart-Smith[3] which was developed on a NASA contract in the early 70's. Those results have been frequently quoted in reports and publications which have appeared since then, and a comparison with the present results is in order. The most crucial part of the Hart-Smith analysis is the expression given for adherend bending, which we may compare with Eq(21.2) of the present analysis. This is repeated here for comparison:

$$\frac{d^2\bar{w}}{dx^2} - \frac{U^2}{8t^2}\bar{w} = \frac{U^2}{8t^2}(\alpha x - \frac{t+t_b}{2}) + \frac{t+t_b}{2}\frac{1}{D_U}\delta_T \qquad (RPT\,21.2)$$

The comparable equation in [4] is equivalent to a twice differentiated version of Eq(35.2)

$$\frac{d^4\bar{w}}{dx^4} - \frac{U^2}{2t^2}\frac{d^2\bar{w}}{dx^2} = \frac{1}{2}(t_b+t)\frac{1}{D_U}\tau_{b,x}$$

but lacking the second order term which is needed to allow for the influence of deflection on moments, ie.

$$\frac{d^4\bar{w}}{dx^4} = \frac{1}{2}(t_b+t)\frac{1}{D_U}\tau_{b,x}$$

The absence of the second derivative term here completely changes the character of the solution. As a result, the influence predicted by this approach gives much longer range effects than those of the present analysis. In effect, this prevents St. Venant's principle from being satisfied in the sense of not allowing Eq(1) to be applicable at any point in the system. of either GR or the present analysis is in the variation of k which is obtained. Table 3 compares the expression for k vs. overlap length obtained from the three approaches.

Considering k as a function of $U\lambda/2 \equiv (12\bar{\varepsilon}_x)^{1/2}\ell/2t$, i.e. dimensionless overlap length together with square root of the loading strain, the GR analysis has the well known asymptotic limit $k \approx 0.262$ for large $U\lambda/2$. The present theory will likewise be found to produce an asymptotic limit but one which may vary to some extent from 0.262, especially for thin adherends. In

TABLE 3 COMPARISON OF EXPRESSIONS FOR k vs. $U\lambda/2$
{ case of $\tanh(U\lambda_o)\approx 1$ }

Goland & Reissner[1] (k_{GR})	$\dfrac{1}{1+\sqrt{8}\tanh\left(\dfrac{U\lambda}{2\sqrt{8}}\right)}$
Hart-Smith[3] (k_{HS})	$\dfrac{1}{1+U\dfrac{\lambda}{2}+\dfrac{1}{6}\left(U\dfrac{\lambda}{2}\right)^2}$
Present Analysis (k_n)	$\dfrac{R_1(1+R^2C_2)+8R_2\dfrac{T_{h21}}{T_{h22}}R(C_1-C_2)}{R_1+8R_2\dfrac{T_{h21}}{T_{h22}}RC_1+\sqrt{8}(1+R^2C_1)T_{h21}}$

where { $Eq(27,28,30,41,44)$ }

$$R\equiv\sqrt{12\frac{\bar{\sigma}_x}{G_b}\frac{t_b}{t}}\quad;\quad R_1=\frac{\sqrt{8\nu_1}}{R}\quad;\quad R_2=\sqrt{\frac{\nu_2}{8}}$$

with $\nu_1,\nu_2=a\pm b\quad;\quad a=\left[4\left(1+\frac{3}{4}\rho_t\right)+\frac{R^2}{4}\right]\quad;\quad b=\sqrt{a^2-R^2}$

and $C_1=\frac{1}{64}\frac{J_1}{J_2}\quad;\quad C_2=\frac{1}{48J_2}\quad;\quad J_1=\frac{1}{R_2^2-\frac{R^2}{16}}\quad;\quad J_2=\frac{R_2^2}{4R_2^2-1}$

contrast, the Hart-Smith expression has lower limit of zero for increasing $U\lambda$. Note that he latter result corresponds to zero shear and peel stresses. This type of behavior is not consistent with what is found in most problems of load diffusion which is what we are dealing with near the end of the overlap, and a lower limit on the stresses which persists even for indefinitely long overlaps and large loads seems to be more in line with practical expectations.

NUMERICAL RESULTS

The degree to which the results of the original Goland and Reissner analysis differ from those of the updated analysis of the present paper depends primarily on the R, the ratio of U to β,

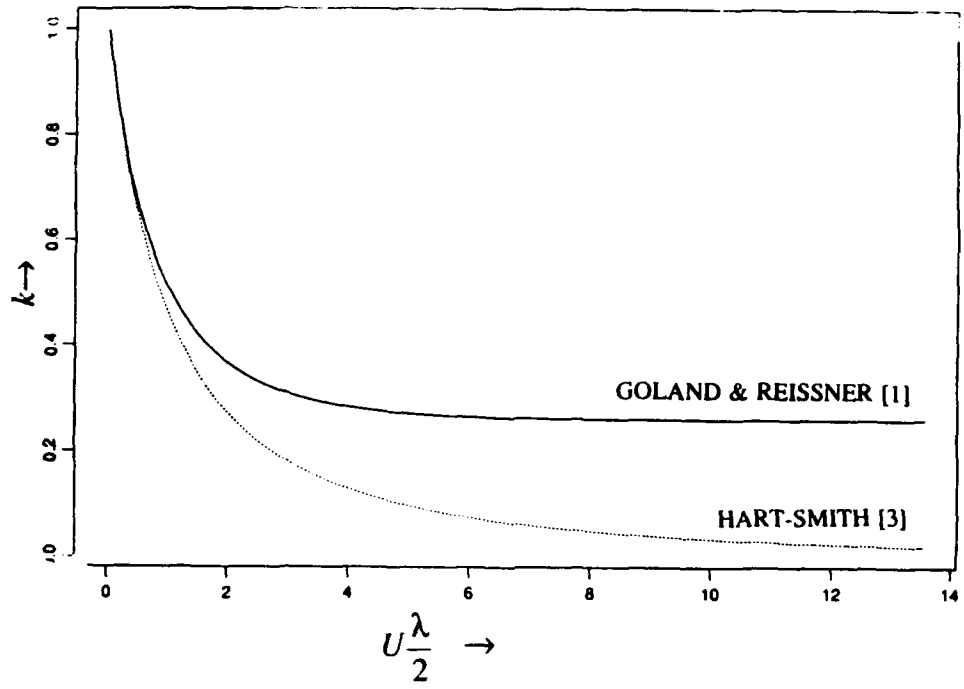

Figure 8 **Comparison of Goland Reissner[1] and Hart-Smith Prediction of k vs. Uλ**

which is equivalent to $(12\bar{\sigma}_x t_b/G_b t)^{1/2}$ according to Eq(27). Results which illustrate the situation are given in Figure 8-10.

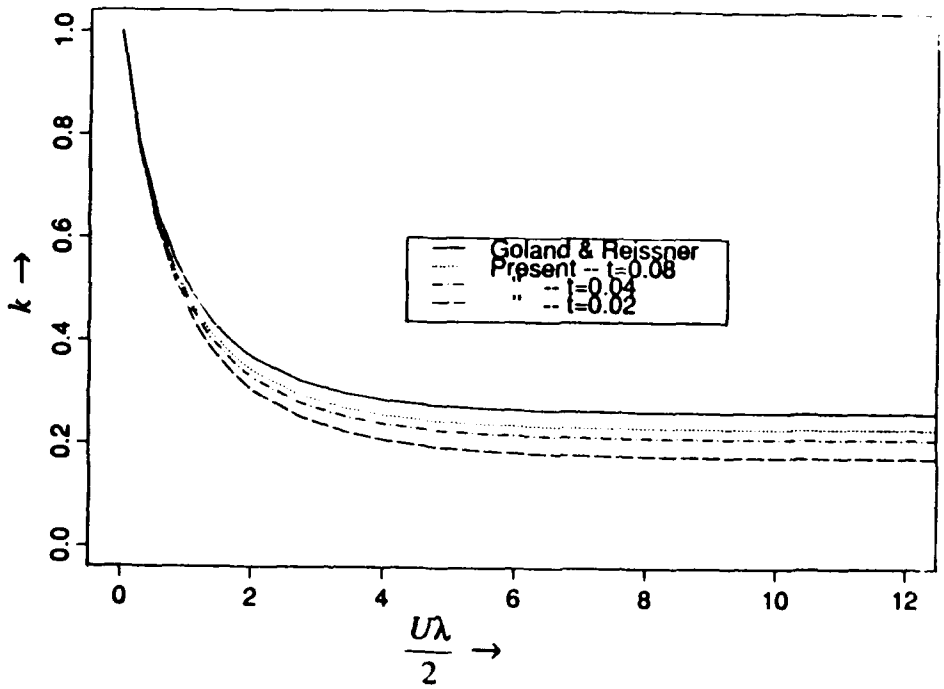

Figure 9 **Comparison of k vs. Uλ Prediction for Goland Reissner vs. Present Theories**

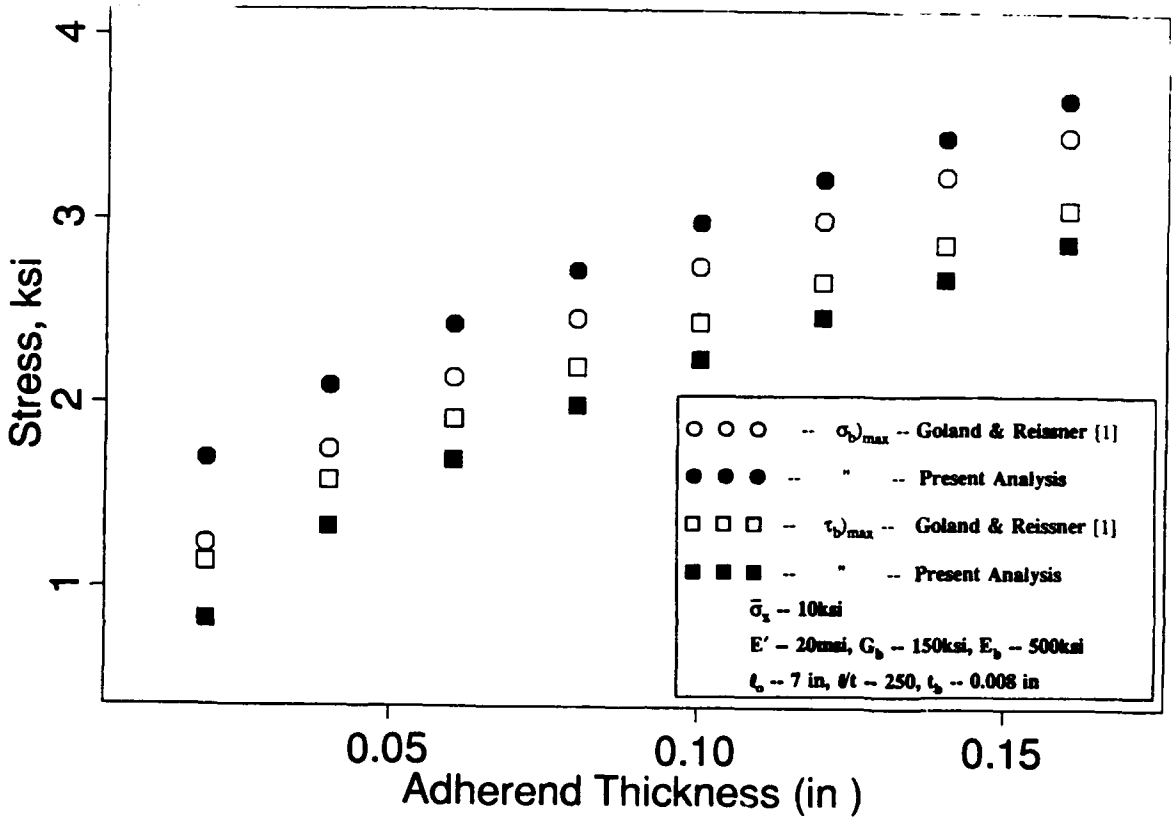

Figure 10 **Comparison of Stress Predictions -- Goland Reissner vs. Present Theories**

Figure 8 gives a comparison of the GR and Hart-Smith predictions for k vs. $U\lambda$, while Figure 9 shows a similar comparison between GR and the results of the present analysis for k vs. $U\lambda$.
The effect of R on the curve of k vs. $U\lambda/2$ is effectively brought out in these results. It is clear that the largest difference between GR and the present analysis occurs for small adherend thicknesses.

Figure 10 shows the effect of adherend thickness on the shear and peel stress predictions obtained from the present analysis for large enough $U\lambda$ so that effects of joint length have settled out, i.e. with k having reached its lower limit. For the case considered here,

$$E' = 20x10_6 \text{ psi}, G_b=150 \text{ ksi}, E_b=500 \text{ ksi}, t_b = 0.008 \text{ in}, \bar{\sigma}_x = 20 \text{ ksi}.$$

It is interesting to note that the ratio of maximum peeling to shear stresses predicted in Eq(15) for the GR analysis is close to unity, so that the GR curves lie nearly on top of each other. Considerable deviation from the GR curves is noted in those of the present analysis. In particular, the shear stresses obtained from the present analysis are greater than those predicted by GR, while the peel stresses are somewhat less than those obtained by GR.

CONCLUSIONS

In the context of the use of beam theory for modelling adherend response, the approach employed in this paper appears to provide the first completely consistent model for the analysis of single lap joints. It is emphasized that the original Goland-Reissner model, in analyzing the deflections of the joint, used a classical homogeneous beam model for calculating deflections which was not consistent with the bi-layer model used by them to predict bond shear and peel stresses. Due to the long-range nature of the effect of bond shear strains on the bending stiffness of the joint when the adherends are thin, the largest differences between the present approach and the GR approach occur the case of thin adherends. On the other hand, the numerical results which have been obtained demonstrate that the original GR approach produces numerical results which do not substantially differ from those of the present analysis. It is clear that for large adherend thicknesses, the effects which are ignored in the original GR approach are so concentrated near the ends of the overlap that their consequences are not significant. Thus for thicker adherends, the GR approach can be considered to have been satisfactory from the stand-point of sound engineering. The insight that Goland and Reissner brought to bear on the effects of adherend bending deflections together with the role of peel stresses on the strength of adhesive joints still stand as a major advance in the understanding of factors important to successful adhesive joint design.

ACKNOWLEDGEMENT

The author is grateful to Dr. L. J. Hart-Smith for a number of discussions and observations regarding the present effort.

APPENDIX A EQUATIONS OF GOLAND REISSNER ANALYSIS

BASIC RELATIONSHIPS

Adherend Constitutive Relations

$$T_U = B_U \frac{du_U}{dx} \quad (A\text{-}1.1) \; ; \qquad T_L = B_L \frac{du_L}{dx} \quad (A\text{-}1.2) \; ; \qquad M_U = D_U \frac{d^2 w_U}{dx^2} \quad (A\text{-}1.3) \; ; \qquad M_L = D_L \frac{d^2 w_L}{dx^2} \quad (A\text{-}1.4)$$

$$D_U \equiv D_L = E' \frac{t^3}{12} \quad (A\text{-}1.5); \qquad B_U \equiv B_L = E' t \quad (A\text{-}1.6)$$

$$E' = E/(1-\nu^2) \; ; \qquad \nu \equiv Poisson's ratio$$

Moment Distribution (Figure 6)

OuterEndofUpperAdherend $(0 < x < \ell_o)$

$$M_U = \bar{T}(\alpha x + w) \qquad (A\text{-}2.1)$$

Moment about Neutral Axis in Overlap Region $(\ell_o < x < \ell_o + \ell)$

$$M_N = \bar{T}\alpha x - (\frac{t}{2} - w)\bar{T} \qquad (A\text{-}2.2)$$

Equilibrium Relations

Upper Adherend Forces *(Fig.A-1(A))*

$$\frac{dT_U}{dx} = \tau_b \quad (A\text{-}3.1) \quad i.e. \quad T_U = \bar{T} + \int_0^x \tau_b dx' \quad (A\text{-}3.2) \; ; \qquad \frac{dV_U}{dx} = \sigma_b \quad (A\text{-}3.3) \quad i.e. \quad V_U = V_o + \int_0^x \sigma_b dx' \quad (A\text{-}3.4)$$

$$\frac{dM_U}{dx} = \frac{t}{2}\tau_b - V_U \quad (A\text{-}3.5) \; ; \qquad d\frac{M_L}{dx} = \frac{t}{2}\tau_b - V_L \quad (A\text{-}3.6)$$

Global Equilibrium in Overlap Region *(Fig.A-1(B))*

$$T_U + T_L = \bar{T} \quad (A\text{-}3.7) \; ; \qquad V_U + V_L = -V_o \quad (A\text{-}3.8)$$

Bond Layer Constitutive and Kinematic Relations

Bond Layer Strains *(Fig.A-2)*

$$\gamma_b = \frac{1}{t_b}[(u_U - u_L) + \frac{t}{2}(w_U x + w_L x)] \qquad (A\text{-}4.1) \; ; \qquad \varepsilon_{zb} = \frac{w_U - w_L}{t_b} \qquad (A\text{-}4.2)$$

BondLayerStresses

$$\tau_b = G_b \gamma_b \qquad (A\text{-}4.3) \; ; \qquad \sigma_b = E_b \varepsilon_{zb} \qquad (A\text{-}4.4)$$

Note that Eq(A-2) exhibit the influence of lateral deflection on the moment distribution due to the shift the lever arm through which the end load, $\bar{T}$, acts with respect to the neutral axis of the adherend segnments under consideration (see Figure 6(A) for the outer adherend and Figure 6(B) and (C) for the overlapping part of the joint.

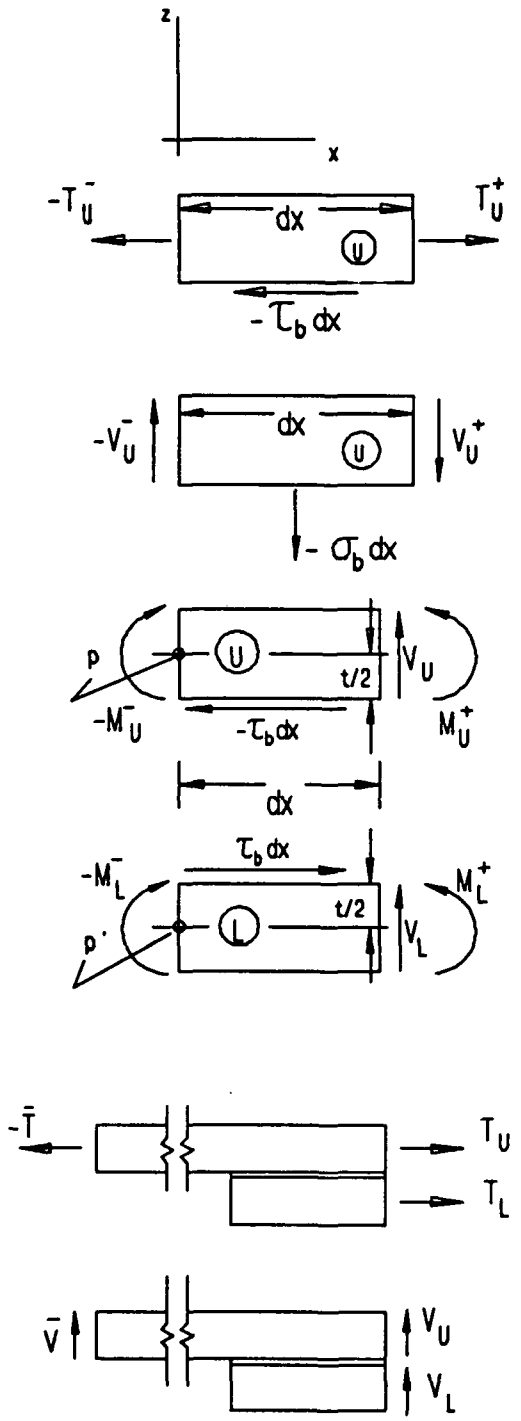

Figure A-1 Equilibrium Relationships

(A) Differential Relationships

$$\sum F_x \equiv T_U^+ + (-T_U^-) - \tau_b dx = 0 \quad \therefore \quad \frac{dT_U}{dx} = \tau_b$$

$$\sum F_z \equiv V_U^+ + (-V_U^-) - \sigma_b dx = 0 \quad \therefore \quad \frac{dV_U}{dx} = 0$$

$$\sum M_U\,(about\ p) \equiv M_U^+ - M_U^- + V_U\,dx - \frac{t}{2}\tau_b dx$$

$$\therefore \frac{dM_U}{dx} = \frac{t}{2}\tau_b - V_U$$

$$\sum M_L\,(about\ p') \equiv M_L^+ - M_L^- + V_L\,dx - \frac{t}{2}\tau_b\,dx$$

$$\therefore \frac{dM_L}{dx} = \frac{t}{2}\tau_b - V_L$$

(B) Global Relationships

$$\sum F_x \equiv T_U + T_L + (-\bar{T}) = 0 \quad \therefore \quad T_U + T_L = \bar{T}$$

$$\sum F_z \equiv V_L + V_U + \bar{V} = 0 \quad \therefore \quad V_U + V_L = -\bar{V}$$

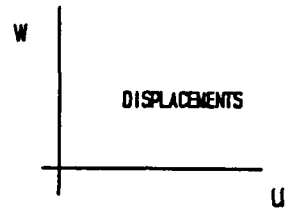

(A) EFFECT OF ADHEREND HORIZONTAL SLIDING

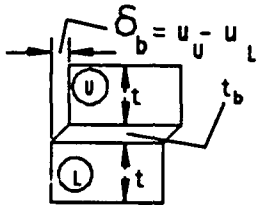

$$\gamma_b \equiv \frac{\delta_b}{t_b} = \frac{u_U - u_L}{t_b}$$

(B) EFFECT OF ADHEREND ROTATION

$$\delta_b = (t + t_b)\tan\Theta \approx t\,\frac{w_U' + w_L'}{2}$$

$$\begin{cases} t/2 \gg t_b \\ w_U \approx w_L \\ dw/dx \equiv w' \approx \tan\Theta \end{cases}$$

$$\gamma_b \equiv \frac{\delta_b}{t_b} \approx \frac{1}{2}\frac{t}{t_b}(w_U' + w_L')$$

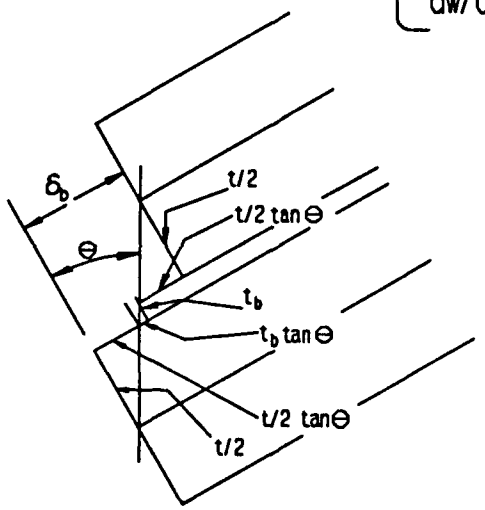

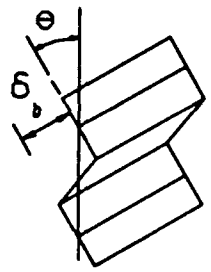

Figure A-2 Bond Layer Shear Strain Components

DIFFERENTIAL EQUATIONS

In the following, the relationships on which the diferential equation under consideration is based are given preceeding the DE's.

Adherend Deflections

Outer Segment of Adherend {*Eq*(A-1.3),(A-2.1)}

$$\frac{d^2w_U}{dx^2} - \frac{U^2}{t^2}w_U = \frac{U^2}{t^2}\alpha x \quad (A\text{-}5.1)$$

Overlapping Segment of Joint {*Eq*(1),(A-2.2)}

$$\frac{d^2w}{dx^2} - \frac{U^2}{8t^2}w = \frac{U^2}{8t^2}(\alpha x - \frac{t}{2}) \quad (A\text{-}5.2)$$

$$\text{where} \quad U = t\sqrt{\frac{\bar{T}}{D_U}} \equiv \sqrt{12\bar{\varepsilon}_x} \quad (A\text{-}5.3)$$

Bond Layer Shear Stress & Strain

Shear Strain {*Eq*(A-4.1),(A-1.1) *to* (A-1.4) *differentiated*, (A-1.5)-(A-1.6)}

$$\frac{d\gamma_b}{dx} = \frac{1}{t_b}[(\frac{T_U}{B_U} - \frac{T_L}{B_L}) + \frac{t}{2}(\frac{M_U}{D_U} + \frac{M_L}{D_L})] \quad (A\text{-}6.1)$$

Shear Stress {*Eq*(A-4.3), (A-1) & (A-6.1) *twice differentiated*, (A-3.5,.6), (A-3.8) *differentiated*}

$$\frac{d^3\tau_b}{dx} - 8\frac{\beta^2}{t^2}\frac{d\tau_b}{dx} = 0 \quad (A\text{-}6.2)$$

$$\text{where } \beta = \sqrt{\rho_G/\rho_t} \quad ; \quad \rho_G = \frac{G_b}{E'} \quad ; \quad \rho_t = \frac{t_b}{t} \quad (A\text{-}6.3)$$

Bond Layer Peel Stress

{*Eq*(A-1.3, .4), (A-3.3), (A-3.5,.6), (A-4.1,.3)}

$$\frac{d\sigma_b^4}{dx^4} + 4\frac{\gamma^4}{t^4}\sigma_b = 0 \quad (A\text{-}7.1)$$

$$\text{where} \quad \gamma = (2\frac{E_b}{D_U t_b})^{1/4} \quad (A\text{-}7.2)$$

SOLUTIONS

Adherend Deflections

In the following, the outer adherend deflection is represented as a multiple of kt/2, corresponding to the notation for M_o given in Eq(A-1). The parameter k is determined by satisfaction of joining conditions between the outer adherend and overlapping part of the joint at $x=\ell_o$.

Generic Expressions

$$\underline{x<\ell_o} \quad w=\frac{kt}{2}\frac{\sinh(Ux/t)}{\sinh(U\lambda_o)}-\alpha x \quad (A-7.1) \qquad \underline{\ell_o<x<\ell_o+\ell} \quad w=W_2\frac{\sinh[(U/\sqrt{8})(x-L)/t]}{\sinh[U\lambda/\sqrt{8}]}+\frac{t}{2}-\alpha x \quad (A-7.2)$$

Continuity Conditions at $x=\ell_o$

$$\underline{\textit{Displacement:}} \quad k\frac{t}{2}=-W_2+\frac{t}{2}-\alpha\ell_o \quad (A-7.3) \quad ; \quad \underline{\textit{Slope:}} \quad k\frac{t}{2}\frac{U}{t}\frac{1}{T_{h1}}=\frac{U}{\sqrt{8}}\frac{W_2}{t}\frac{1}{T_{h2}} \quad (A-7.4)$$

Resulting Expressions

$$W_2=\frac{t}{2}(1-k) \quad (A-7.5) \quad ; \quad k=\frac{T_{h1}}{T_{h1}+\sqrt{(}8)T_{h2}} \quad (A-7.6) \quad ; \quad k'=\frac{1}{4T_{h1}}k\lambda U \quad (A-7.7)$$

where $\quad T_{h1}=\tanh(U\lambda_o) \quad (A-7.8) \quad ; \quad T_{h2}=\tanh(U\lambda/2\sqrt{8}) \quad (A-7.9)$

Note that GR assume the outboard part of the adherend to be long enough to make $U\lambda>>1$, leading to $T_{h1}\approx 1$, as a result of which they use the contracted expressions

$$k=\frac{1}{1+\sqrt{8}T_{h2}} \quad ; \quad k'=\frac{1}{4}k\lambda U \quad (A-8)$$

for k and k′.

Bond Layer Shear Stress

Generic Solution of Eq(A-6.2)

$$\tau_b=c_1e^{\sqrt{8}\,\beta\frac{(x-L)}{t}}+c_2e^{-\sqrt{8}\,\beta\frac{(x-L)}{t}}+const. \qquad (A-9)$$

Bond Layer Shear Stress (cont)

Boundary Conditions

(1) *Using Eq(A-6.1) multiplied by G_b to generate $d\tau_b/dx$, end conditions determined by M_U, M_L, T_U and T_L, inserted on RHS of (A-6.1).*

(2) *Determine const. in (A-9) by integrating $\tau_b x$ then inserting into (A-3.2) to satisfy $T_U=0$ condition at $x=L+\ell$*

Final Form of Solution

$$\tau_b = -\bar{\sigma}_x[\sqrt{2}\beta\frac{(1+3k)}{4}\frac{\cosh[\sqrt{8}\beta(x-L)/t]}{\sinh\sqrt{8}\beta\lambda}+\frac{3}{4\lambda}(1-k)] \qquad (A-10.1)$$

Maximum Value of τ_b *($x=L\pm\ell/2$; $\sqrt{8}\beta\lambda/2>1$; $0.262<k<1$)*

$$0.631\beta \;<\; abs\{\frac{\tau_b)_{max}}{\bar{\sigma}_x}\} \approx \sqrt{2}\beta\frac{(1+3k)}{4} \;<\; 1.414\beta \qquad (A-10.2)$$

Peel Stresses

Functional Notation

$$Cc(x) = \cosh(\gamma\frac{x-L}{t})\cos(\gamma\frac{x-L}{t}) \quad (A-11.1) \qquad Ss(x) = \sinh(\gamma\frac{x-L}{t})\sin(\gamma\frac{x-L}{t}) \quad (A-11.2)$$

$$Sc(x) = \sinh(\gamma\frac{x-L}{t})\cos(\gamma\frac{x-L}{t}) \quad (A-11.3) \qquad Cs(x) = \cosh(\gamma\frac{x-L}{t})\sin(\gamma\frac{x-L}{t}) \quad (A-11.4)$$

Derivative Relationships

$$(Cc)' = \frac{\gamma}{t}(Sc-Cs) \quad (A-12.1) \qquad (Ss)' = \frac{\gamma}{t}(Sc+Cs) \quad (A-12.2)$$

$$(Cc)'' = -2\frac{\gamma^2}{t^2}Ss \quad (A-12.3) \qquad (Ss)'' = 2\frac{\gamma^2}{t^2}Cc \quad (A-12.4)$$

Generic Solution *(σ_c, σ_s, --constants determined by boundary conditions)*

$$\sigma_b(x) = \sigma_c Cc + \sigma_s Ss \quad (A-13)$$

Boundary Conditions

(1) *Eq*(A-4.2) *combined with* (A-4.1) *differentiated twice* (*making use of* (A-1.3, ,4)):

$$\frac{d^2\sigma_b}{dx^2} = \frac{E_b}{t_b}\frac{M_U - M_L}{D_U} \qquad (A-14.1)$$

(2) *Differentiation of* (A-14.1), *making use of* (A-3.5,.6):

$$\frac{d^3\sigma_b}{dx^3} = -\frac{E_b}{t_b}\frac{V_U - V_L}{D_U} \qquad (A-14.2)$$

(For $x=\ell_o$ and $\ell+\ell_o$, differenced quantities appearing on the RHS of Eq(A-14) are taken from the last two rows of Table 2.)

ResultingExpressions

$$\sigma_b(x) = \frac{1}{\Delta}\frac{\bar{T}\gamma}{t}\{(P_2\frac{1}{2}\frac{k\gamma}{t} + \frac{2}{\lambda}k'P_4)Cc(x) + (P_1\frac{1}{2}\frac{k\gamma}{t} + \frac{2}{\lambda}k'P_3)Ss(x)\} \qquad (A-15.1)$$

where

$$P_1 = (Sc+Cs)_{(x-L)/t=\lambda/2} \quad P_2 = (Sc-Cs)_{(x-L)/t=\lambda/2} \quad P_3 = Ss_{(x-L)/t=\lambda/2} \quad p4 = Cc_{(x-L)/t=\lambda/2}$$

$$\Delta = (P_1P_4 - P_2P_3)_{(x-L)/t=\lambda/2} \qquad (A-15.2)$$

Maximum Value of Peel Stress ($x = L \pm \ell/2$; $\gamma\lambda/2 > 1$)

Note that (*Eq*(A-8)) $\quad \frac{2k'}{\lambda} = \frac{kU}{2}$

$$\therefore \textit{For } x = L \pm \ell/2 \;;\; \sigma_b = \bar{\sigma}_x\gamma\{\frac{k\gamma}{2}\frac{(P_2P_4 + P_1P_3)}{\Delta} + \frac{kU}{2}\frac{(P_4^2 + P_3^2)}{\Delta}\}$$

Also, for $\gamma\lambda/2 > 1$; $\frac{P_2P_4 + P_1P_3}{\Delta} \approx \frac{P_3^2 + P_4^2}{\Delta} \approx 1$

$$\therefore \qquad \sigma_b)_{max} \approx \bar{\sigma}_x\frac{k\gamma}{2}(\gamma + U) \qquad (A-15.3)$$

APPENDIX B
PEEL STRESS SOLUTION IN UPDATED ANALYSIS

Notation pertinent to this section are given in Table B.1. Eq(66) which defines the peel stresses is repeated here for reference:

$$\frac{d^4\sigma_b}{dx^4} - \frac{U^2}{2t^2}\frac{d^2\sigma_b}{dx^2} + \frac{4\gamma^4}{t^4}\sigma_b = Q(x) \qquad (B\text{-}1.1)$$

where

$$Q(x) = \delta_T(x)\bar{w}''(x) \qquad (B\text{-}1.2)$$

It is noted that the factors included in the function Q(x), on the right side of (B-1.1), involve only the homogeneous parts of the solutions for δ_T and $\bar{w}(x)$, so that (B-1.2) can be written

$$Q(x) = \{\Delta_{h1}\frac{\sinh[\mu_1(x-L)/t]}{\sinh(\mu_1\lambda/2)} + \Delta_{h2}\frac{\sinh[\mu_2(x-L)/t]}{\sinh(\mu_2\lambda/2)}\}$$

$$\times \quad \{\frac{\mu_1^2}{t^2}k_{21}\frac{t}{2}\frac{\sinh[\mu_1(x-L)/t]}{\sinh(\mu_1\lambda/2)} + \frac{\mu_2^2}{t^2}k_{22}\frac{t}{2}\frac{\sinh[\mu_2(x-L)/t]}{\sinh(\mu_2\lambda/2)}\} \qquad (B\text{-}2)$$

Defining $\bar{M}$ together with the q_{ij}'s (i,j = 1,2) as in Table B-1 and noting that from the definition of $\bar{M}$ and U, we have that

$$\frac{\bar{M}U^2}{8t^2} = \frac{3}{4}\bar{\sigma}_x\bar{\varepsilon}_x \qquad (B\text{-}3)$$

then using appropriate identities for the hyperbolic functions in (B-2) together with the functional notation in Table B-1 leads to

$$Q(x) = \frac{3}{4}\bar{\sigma}_x\bar{\varepsilon}_x\{q_{11}\frac{F_{11}(\xi)-1}{F_{11}(\lambda/2)-1} + q_{22}\frac{F_{22}(\xi)-1}{F_{22}(\lambda/2)-1} + q_{12}\frac{F_{21}(\xi)-F_{12}(\xi)}{F_{21}(\lambda/2)-F_{12}(\lambda)}\} \qquad (B\text{-}4)$$

Equation (B-1.1) can then be expressed as a sum of terms for each of which the RHS of (B-1.1) is an exponential function, giving a differential equation of the type

$$\frac{d^4\sigma_b}{dx^4} - \frac{U^2}{t^2}\frac{d^2\sigma_b}{dx^2} + \frac{4\gamma^4}{t^4}\sigma_b = \frac{2\gamma^4}{t^4}Fe^{\alpha x/t} \qquad (B\text{-}5)$$

where α and F are constants. Eq(B-5) has the particular solution

$$\sigma_p = \frac{1}{\frac{\alpha^4 - U^2\alpha^2 + 4\gamma^4}{2\gamma^4} + 2}Fe^{\alpha x/t} \qquad (B\text{-}6)$$

Decomposing the right side of (B-1.1) into exponential terms and repeatedly applying (B-6) gives the particular solution that is needed here. The homogeneous solution of (B-1.1) consists of terms of the form

$$\sigma_b = \sigma_{h1}e^{\gamma_i x/t}\cos(\gamma_i x/t) + \sigma_{h2}e^{\gamma_i x/t}\sin(\gamma_i x/t)$$

$$+ \sigma_{h3}e^{-\gamma_i x/t}\cos(\gamma_i x/t) + \sigma_{h4}e^{-\gamma_i x/t}\sin(\gamma_i x/t) \qquad (B\text{-}7)$$

TABLE B-1 NOTATION FOR PEEL STRESS EXPRESSIONS

PARAMETRIC NOTATION

General

$$\bar{M} = t\frac{\bar{T}}{2} \equiv \bar{\sigma}_x \frac{t^2}{2} \quad ; \quad \xi = \frac{(x-L)}{t}$$

Definition of g_{ij}'s

$$q_{11} = \frac{\Delta_{h1}\frac{\mu_1^2}{t^2}k_{21}\frac{t}{2}}{\bar{M}\frac{U^2}{8t^2}} \quad i.e. \quad q_{11}\bar{M}\frac{U^2}{t^2} = \Delta_{h1}\frac{\mu_1^2}{t^2}k_{21}\frac{t}{2} \quad ; \quad q_{22} = \frac{\Delta_{h2}\frac{\mu_2^2}{t^2}k_{22}\frac{t}{2}}{\bar{M}\frac{U^2}{8t^2}} \quad i.e. \quad q_{22}\bar{M}\frac{U^2}{t^2} = \Delta_{h2}\frac{\mu_2^2}{t^2}k_{22}\frac{t}{2}$$

$$q_{12} = \frac{\Delta_{h1}\frac{\mu_1^2}{t^2}k_{21}\frac{t}{2} + \Delta_{h2}\frac{\mu_2^2}{t^2}k_{22}\frac{t}{2}}{\bar{M}\frac{U^2}{t^2}} \quad i.e. \quad q_{12}\bar{M}\frac{U^2}{t^2} = \Delta_{h1}\frac{\mu_1^2}{t^2}k_{21}\frac{t}{2} + \Delta_2\frac{\mu_2}{t^2}k_{22}\frac{t}{2}$$

q_{ij}s IN TERMS OF NOTATION OF EQ(39.3, .4), (52.2), (54)

$$q_{11} = -\frac{3}{4}J_1 k_{21}^2 R_1^2 \quad ; \quad q_{22} = \frac{4R_2^2}{3J_2}\left(\frac{3}{4}J_1 k_{21} - 1\right)^2 \quad ; \quad q_{12} = \left(-\frac{J_1}{J_2}R_2^2 + R_1^2\right)\left(\frac{3}{4}J_1 k_{21} - 1\right)k_{21}$$

Definition of D_{ij}s

$$D_{11} = \frac{\mu_1^4 - U^2\mu_1^2}{2\gamma^4} + 2 \quad ; \quad D_{22} = \frac{\mu_2^4 - U^2\mu_2^2}{2\gamma^4} + 2 \quad ; \quad D_{12} = \frac{(\mu_1+\mu_2)^4 - U^2(\mu_1+\mu_2)^2}{2\gamma^4} + 2 \quad ; \quad D_{21} = \frac{(\mu_2-\mu_1)^4 - U^2(\mu_2-\mu_1)^2}{2\gamma^4} + 2$$

FUNCTIONAL NOTATION

$$F_{11}(\xi) = \cosh 2\mu_1\xi \quad ; \quad F_{22}(\xi) = \cosh 2\mu_2\xi \quad ; \quad F_{12}(\xi) = \cosh(\mu_1-\mu_2)\xi \quad ; \quad F_{21}(\xi) = \cosh(\mu_1+\mu_2)\xi$$

$$G_{11} = \sinh 2\mu_1\xi \quad ; \quad G_{22}(\xi) = \sinh 2\mu_2\xi \quad ; \quad G_{12}(\xi) = \sinh(\mu_1+\mu_2)\xi \quad ; \quad G_{21}(\xi) = \sinh(\mu_1+\mu_2)\xi$$

in which $\pm(\gamma_r \pm i\gamma_i)$ [$i=(-1)^{1/2}$] are complex roots of the quartic polynomial

$$z^4 - U^2 z^2 + 4\gamma^4 = 0 \qquad (B\text{-}8)$$

associated with (B-1.1). The solution to (B-8) is

$$z^2 \equiv [\pm(\gamma_r \pm i\gamma_i)]^2 = \pm[\frac{U^2}{2} \pm i\sqrt{(4\gamma^4 - \frac{1}{4}U^4)}\,] \qquad (B\text{-}9)$$

Because of the second derivative appearing in (B-1.1), it is found that γ_r γ_i, in contrast with the original GR solution. However, the contribution of terms involving U in (B-9) compared with those involving γ is miniscule, and can be ignored with no risk of significant inaccuracy. Thus the homogeneous part of the peel stress solution is essentially in agreement with that of the GR solution will now be

$$\sigma_p = \sigma_{bp} + \sigma_{bh} \qquad (B\text{-}10)$$

where the homogeneous term, σ_{bh}, is now assumed to have the same form as that of Eq(A-14) of the GR analysis of Appendix A

$$\sigma_{bh} = \sigma_c Ss + \sigma_s Cc \qquad (B\text{-}11)$$

but with σ_c and σ_s appropriately modified:

$$\sigma_c = \frac{P_2\frac{2\gamma^2}{t^2}(M_o - M_p) + P_4\frac{2\gamma^2}{t^2}(V_o - V_p)}{\Delta} \quad ; \quad \sigma_p = \frac{P_1\frac{2\gamma^2}{t^2}(M_o - M_p) + P_3\frac{2\gamma^2}{t^2}(V_o - V_p)}{\Delta} \qquad (B\text{-}12)$$

in which M_0 and V_o are as before given in (A-13) which may be re-expressed here for convenience, using notation which has been introduced in Appendis A (assuming $T_{h1}\approx 1$ in (A-13.2)) as

$$M_o = k_a \bar{\sigma}_x \frac{t^2}{2} \quad ; \quad V_o = k_a \bar{\sigma}_x t\sqrt{3\bar{\varepsilon}_x} \qquad (B\text{-}13)$$

while M_p and V_p are obtained from derivatives of σ_{bp}, i.e.:

$$M_p = -\frac{t^4}{2\gamma^4}\frac{d^2\sigma_{bp}}{dx^2} \quad ; \quad V_p = \frac{t^4}{2\gamma^4}\frac{d^3\sigma_{bp}}{dx^3} \qquad (B\text{-}14)$$

The in the notation of Table B-1, the particular solution to Eq(B-1) is

$$\sigma_{bp} = \frac{3}{2}\bar{\sigma}_x\bar{\varepsilon}_x\{\frac{q_{11}}{D_{11}}\frac{F_{11}(\xi)-1}{F_{11}(\lambda/2)-1} + \frac{q_{22}}{D_{22}}\frac{F_{22}(\xi)-1}{F_{22}(\lambda/2)-1} + \frac{\frac{q_{12}}{D_{21}}F_{21}(\xi) - \frac{q_{21}}{D_{12}}F_{12}(\xi)}{F_{11}(\lambda/2)-F_{12}(\lambda/2)}\} \qquad (B\text{-}15)$$

Derivatives of σ_{bp} required to evaluat (B-15) are then given by

At this point we wish to concentrate on evaluating quantities of interest at $(x-L)/t = \lambda/2$ where the boundary conditions are applied. We also assume the case of long overlap for which $\mu_1\lambda$, $\mu_2\lambda$ >>1. In such cases all functionaL ratios in (B-16) can be replaced by unity. The defining allows M_p and V_p to be expressed as

$$M_p = -\frac{3}{16}Gt^2\bar{\sigma}_x\bar{\varepsilon}_x \quad ; \quad V_p = \frac{3}{2}Ht\bar{\sigma}_x\bar{\varepsilon}_x \qquad (B\text{-}19)$$

$$\frac{d^2\sigma_{bp}}{dx^2} = \frac{3}{2}\bar{\sigma}_x\bar{\varepsilon}_x\{4\mu_1^2\frac{q_{11}}{D_{11}}\frac{F_{11}(\xi)}{F_{11}(\lambda/2)-1} + 4\mu_2^2\frac{q_{22}}{D_{22}}\frac{F_{22}(\xi)}{F_{22}(\lambda/2)-1}$$

$$+\frac{(\mu_2+\mu_1)^2\frac{q_{12}}{D_{21}}F_{21}(\xi)-(\mu_2-\mu_1)^2\frac{q_{21}}{D_{12}}F_{12}(\xi)}{F_{11}(\lambda/2)-F_{12}(\lambda/2)}\} \quad (B-16)$$

$$\frac{d^3\sigma_{bp}}{dx^3} = \frac{3}{2}\bar{\sigma}_x\bar{\varepsilon}_x\{8\mu_1^3\frac{q_{11}}{D_{11}}\frac{F_{11}(\xi)}{F_{11}(\lambda/2)-1} + 8\mu_2^3\frac{q_{22}}{D_{22}}\frac{F_{22}(\xi)}{F_{22}(\lambda/2)-1}$$

$$+\frac{(\mu_2+\mu_1)^3\frac{q_{12}}{D_{21}}F_{21}(\xi)-(\mu_2-\mu_1)^3\frac{q_{21}}{D_{12}}F_{12}(\xi)}{F_{11}(\lambda/2)-F_{12}(\lambda/2)}\} \quad (B-17)$$

$$G = \{2\frac{\mu_1^2}{\gamma^4}\frac{q_{11}}{D_{11}} + 2\frac{\mu_2^2}{\gamma^4}\frac{q_{22}}{D_{22}} + \frac{q_{12}}{4\gamma^4}[\frac{(\mu_2-\mu_1)^2}{D_{21}} - \frac{(\mu_1+\mu_2)^2}{D_{12}}]\}$$

$$H = \{4\frac{\mu_1^3}{\gamma^4}\frac{q_{11}}{D_{11}} + 4\frac{\mu_2^3}{\gamma^4}\frac{q_{22}}{D_{22}} + \frac{q_{12}}{4\gamma^4}[\frac{(\mu_2-\mu_1)^3}{D_{21}} - \frac{(\mu_1+\mu_2)^3}{D_{12}}]\} \quad (B-18)$$

and comparing (B-13) with (B-18) gives M_p and V_p as the following ratios with respect to M_o and V_o

$$\frac{M_p}{M_o} \approx \frac{3}{8k_n}G\bar{\varepsilon}_x \quad ; \quad \frac{V_p}{V_o} \approx \frac{\sqrt{3\bar{\varepsilon}_x}}{2k_n}H \quad (B-20)$$

The values of these ratios give a yardstick for judging how significant are the effects of the particular solution on the peel stresses. Numerical evaluation indicates that G and H are on the order of 1 to 2. Assuming the Goland Reissner limit for k ($\approx$0.262) applied to k_n (considering the long overlap case) and a value of 1 for G and H thus indicates that

$$\frac{M_p}{M_o} \approx 0.1\bar{\varepsilon}_x \quad ; \quad \frac{V_p}{V_o} \approx 0.22(\bar{\varepsilon}_x)^{1/2}$$

The adherend strain level will certainly not be greater than 0.01, so that the effect of the particluar solution on the peel stresses is essentially negligible.

DISTRIBUTION LIST

No. of Copies	To
1	Office of the Under Secretary of Defense for Research and Engineering The Pentagon Washington, DC 20301
	Commander U.S. Army Laboratory Command 2800 Powder Mill Road Adelphi, MD 20783-1145
1	ATTN: AMSLC-IM-TL
1	AMSLC-CT
1	AMSLC-TP-TS, J. P. Forry
	Commander Defense Technical Information Center Cameron Station, Building 5 5010 Duke Street Alexandria, VA 22304-6145
2	ATTN: DTIC-FDAC
	Metals and Ceramics Information Center Battelle Columbus Laboratories 505 King Avenue Columbus, OH 43201
1	ATTN: MIAC/CINDAS, Perdue University 2595 Yeager Road, West Lafayette, IN 47905
	Commander Army Research Office P.O. Box 12211 Research Triangle Park, NC 27709-2211
1	ATTN: Information Processing Office
	Commander U.S. Army Materiel Command 5001 Eisenhower Avenue Alexandria, VA 22333
1	ATTN: AMSCI
	Commander U.S. Army Materiel Systems Analysis Activity Aberdeen Proving Ground, MD 21005
1	ATTN: AMXSY-MP, H. Cohen
	Commander U.S. Army Missile Command Redstone Scientific Information Center Redstone Arsenal, AL 35898-5241
1	ATTN: AMSMI-RD-CS-R/Doc
1	AMSMI-RLM
	Commander U.S. Army Armament, Munitions and Chemical Command Dover, NJ 07801
1	ATTN: Technical Library
1	AMDAR-LCA, Harry E. Pebly, Jr. PLASTEC, Director
	Commander U.S. Army Natick Research, Development, and Engineering Center Natick, MA 01760-5010
1	ATTN: Technical Library
	Commander U.S. Army Satellite Communications Agency Fort Monmouth, NJ 07703
1	ATTN: Technical Document Center
	Commander U.S. Army Tank-Automotive Command Warren, MI 48397-5000
1	ATTN: AMSTA-ZSK
1	AMSTA-TSL, Technical Library
	Commander White Sands Missile Range, NM 88002
1	ATTN: STEWS-WS-VT
	President Airborne, Electronics and Special Warfare Board Fort Bragg, NC 28307
1	ATTN: Library
	Director U.S. Army Ballistic Research Laboratory Aberdeen Proving Ground, MD 21005
1	ATTN: SLCBR-TSB-S (STINFO)
	Commander Dugway Proving Ground Dugway, UT 84022
1	ATTN: Technical Library, Technical Information Division
	Commander Harry Diamond Laboratories 2800 Powder Mill Road Adelphi, MD 20783
1	ATTN: Technical Information Office
	Director Benet Weapons Laboratory LCWSL, USA AMCCOM Watervliet, NY 12189
1	ATTN: AMSMC-LCB-TL
1	AMSMC-LCB-R
1	AMSMC-LCB-RM
1	AMSMC-LCB-RP
1	SMCAR-CCB-RT, Glenn Friar
	Commander U.S. Army Foreign Science and Technology Center 220 7th Street, N.E. Charlottesville, VA 22901-5396
3	ATTN: AIFRTC, Applied Technologies Branch, Gerald Schlesinger

No. of Copies	To

Commander
U.S. Army Aeromedical Research Unit
P.O. Box 577
Fort Rucker, AL 36360
1 ATTN: Technical Library

Commander
U.S. Army Aviation Systems Command
Aviation Research and Technology Activity
Aviation Applied Technology Directorate
Fort Eustis, VA 23604-5577
1 ATTN: SAVDL-E-MOS
1 ARTA (AVSCOM), SAVRT-TR-ATS, Barry Spigel

U.S. Army Aviation Training Library
Fort Rucker, AL 36360
1 ATTN: Building 5906-5907

Commander
U.S. Army Agency for Aviation Safety
Fort Rucker, AL 36362
1 ATTN: Technical Library

Commander
USACDC Air Defense Agency
Fort Bliss, TX 79916
1 ATTN: Technical Library

Commander
U.S. Army Engineer School
Fort Belvoir, VA 22060
1 ATTN: Library

Commander
U.S. Army Engineer Waterways Experiment Station
P.O. Box 631
Vicksburg, MS 39180
1 ATTN: Research Center Library

Commandant
U.S. Army Quartermaster School
Fort Lee, VA 23801
1 ATTN: Quartermaster School Library

Naval Research Laboratory
Washington, DC 20375
1 ATTN: Code 5830
1 Code 6384, Dr. G. R. Yoder

Chief of Naval Research
Arlington, VA 22217
1 ATTN: Code 471

1 Edward J. Morrissey
WRDC/MLTE
Wright-Patterson Air Force Base, OH 45433-6523

No. of Copies	To

Commander
U.S. Air Force Wright Research & Development Center
Wright-Patterson Air Force Base, OH 45433-6523
1 ATTN: WRDC/MLLP, M. Forney, Jr.
1 WRDC/MLBC, Stanley Schulman
1 WRDC/MLSE, Neal Ontko
1 WRDC/MLSE, David C. Watson

NASA
Marshall Space Flight Center
MSFC, AL 35812
1 ATTN: Paul Schuerer/EH01

U.S. Department of Commerce
National Institute of Standards and Technology
Gaithersburg, MD 20899
1 ATTN: Stephen M. Hsu, Chief
Ceramics Division, Institute for
Materials Science and Engineering

1 Committee on Marine Structures
Marine Board
National Research Council
2101 Constitution Avenue, N.W.
Washington, DC 20418

1 The Charles Stark Draper Laboratory
68 Albany Street
Cambridge, MA 02139

Wyman-Gordon Company
Worcester, MA 01601
1 ATTN: Technical Library

Lockheed-Georgia Company
86 South Cobb Drive
Marietta, GA 30063
1 ATTN: Materials and Processes Engineering, Dept. 71-11, Zone 54

General Dynamics
Convair Aerospace Division
P.O. Box 748
Fort Worth, TX 76101
1 ATTN: Mfg. Engineering Technical Library

Hercules, Inc.
P.O. Box 98
Magna, UT 84102
1 ATTN: Dr. Mohamed G. Abdaallah, MS 2343-C
1 Gary Hansen

Tiodize Company, Inc.
5858 Engineer Drive
Huntington Beach, CA 92649
1 ATTN: Thomas R. Adams
1 Gary R. Wittman

No. of Copies	To
	Sikorsky Aircraft
	6900 Main Street
	Stratford, CT 06497
2	ATTN: John Adelmann
1	Samuel P. Garbo, Div. of UTC
	Martin Marietta-Aero & Naval Systems
	103 Chesapeake Park Plaza
	Baltimore, MD 21220
1	ATTN: Ms. Karen Albrecht
1	John Ruth
	U.S. Army Aviation Systems Command (ARTA)
	Langley Research Center, MS-190
	Hampton, VA 23665-5225
2	ATTN: Donald Baker
	B. P. Chemicals, Fibers & Materials HITCO
	700 E. Dyer Road
	Santa Ana, CA 92705
1	ATTN: F. C. Bancroft
	DOW/UT Composite Products
	6900 Main Street
	Stratford, CT 06601-1381
2	ATTN: William Beck
1	Dean Nguyen
1	William G. Degnan, MS: S522A
	Hexcel
	11711 Dublin Boulevard
	Dublin, CA 94526
1	ATTN: Tom Bitzer
	Honeywell, Inc.
	Armament Systems Division
	7225 Northland Drive
	Brooklyn Park, MN 55428
1	ATTN: Dr. John H. Bode
	McDonnell Douglas Helicopter Co.
	5000 E. McDowell Road
	Mesa, AZ 85205
1	ATTN: Gregg R. Bogucki, B531/MS C235
1	John Schibler
	McDonnell Douglas Aircraft Company
	P.O. Box 516
	St. Louis, MO 63166-0516
2	ATTN: Raymond E. Bohlmann
	Materials Sciences Corporation
	930 Harvest Drive, Suite 300
	Blue Bell, PA 19422
1	ATTN: Librarian
2	Patrick Brady
1	Dr. Ronald B. Bucinell
1	Dr. Sailendra Chatterjee
1	Dr. Robert Henstenburg
1	Dr. Crystal Newton

No. of Copies	To
	Scion Design Group
	1482 Calabazas Boulevard
	Santa Clara, CA 95051
1	ATTN: Charles L. Brown, III
	Cherry Textron
	1224 E. Warner Avenue
	Santa Ana, CA 92707-0157
1	ATTN: William J. Busch, Jr.
	Boeing Commercial
	P.O. Box 3707
	Seattle, WA 98124
2	ATTN: Dominic J. Calderone
1	Ray Horton, MS 4H-30
1	Ron Zabora, MS 9R-62
	Thiokol Corp, Strategic Opns
	P.O. Box 689, M/S:M51
	Brigham City, UT 84302-0689
2	ATTN: David Cannon
	David Taylor Research Center
	Annapolis, MD 21402
1	ATTN: Gene Camponeschi, Code 2802
1	Terry Morton
	C3 International
	3347 Knollridge Drive
	El Dorado Hills, CA 95630
1	ATTN: Leslie Cooke
	Instron Corporation/Los Angeles
	10377 Los Alamitos Boulevard
	Los Angeles, CA 90720
1	ATTN: Arthur E. Cozens
	Douglas Aircraft Company
	3855 Lakewood Blvd
	Long Beach, CA 90846
1	ATTN: Mervin A. Danforth, MC 36-14
1	Dr. L. J. Hart-Smith
	Gulfstream Aerospace
	P.O. Box 2206
	Savannah, GA 31402-2206
1	ATTN: Curtis Davies
	3M Company, Aerospace Matls Dept
	3M Center, Bldg 230-1F-02
	St. Paul, MN 55144
1	ATTN: J. William Davis
	ICI Fiberite
	2055 E. Technology Circle
	Tempe, AZ 85284
1	ATTN: Eric Derbyshire

No. of Copies	To
	Lockheed Aeronautical Systems Co. D72-37/B-311/Plant B-6/Box 551 Burbank, CA 91520-7237
1	ATTN: John N. Dickson
	Allied-Signal Aero Co/AiRes LA Div 2525 West 190th Street Box 2960 Torrance, CA 90509-2960
1	ATTN: Christopher Duncan
	U.S. Army Cold Regions Laboratory Hanover, NH 03755
1	ATTN: Dr. Piyush Dutta
	Rockwell Intl. Space Systems Division 12214 Lakewood Boulevard Downey, CA 90241
1	ATTN: Alan Fabry
	LTV Aerospace & Defense P.O. Box 655907 Dallas, TX 75265
1	ATTN: James Foster, M/S 194-51
1	Steven Jackson, M/S 194-26
	General Electric Aircraft Engines One Neumann Way MD H85 Cincinnati, OH 45215-6301
1	ATTN: Frank S. Gruber
	Lord Coporation 1S35 West 12th Street Erie, PA 16514
1	ATTN: Dr. B. P. Gupta
	Bentley Harris 241 Welsh Pool Road Lionville, PA 19353
1	ATTN: Joseph P. Hess
	University of Wisconsin 1226 Brookwood Road Madison, WI 53711
1	ATTN: Dr. Bernard Harris
	U.S. Army Aviation Systems Command AMSAV-EFM 4300 Goodfellow Boulevard St. Louis, MO 63120-1798
1	ATTN: Philip Haselbauer
	Steeger USA, Inc. P.O. Box 16040 Spartanburg, SC 29316
1	ATTN: John Hasler

No. of Copies	To
	Boeing Aerospace P.O. Box 3999 M.S. 2A-64 Seattle, WA 98124
1	ATTN: A. B. Hunter
	SPS Technologies Highland Avenue Jenkintown, PA 19046
1	ATTN: Scott Hutchinson
	Ciba Geigy Composite Materials 5115 East La Palma Anaheim, CA 92807-2018
1	ATTN: T. F. Jonas
	Northrop Aircraft Division One Northrop Avenue 3853/82 Hawthorne, CA 90250
1	ATTN: Dr. Han-Pin Kan
	Albany International 777 West Street Mansfield, MA 02048-9114
1	ATTN: Ms. Sheila A. Kavanah
	University Of Wyoming Comp. Matls. Res. Gr. Dept. of Mech. Eng. P.O. Box 3295 Laramie, WY 82071
1	ATTN: Jeff A. Kessler
	Dupont CRP 702, Rm 2319 Chestnut Run Wilmington, DE 19880-0702
1	ATTN: Dr. Subhotosh Khan
	Beech Aircraft P.O. Box 85 M.S. 90B7 Wichita, KS 67201
1	ATTN: Mrs. Ann Kolarik
	U.S. Polymeric 700 East Dyer Road Santa Ana, CA 92707
1	ATTN: Ted Kruhmin
	Phillips 66 1699 W. Adams Boulevard Bartlesville, OK 74004
1	ATTN: Patrick Kunc
	Michigan Technological University ME-EM Department Houghton, MI 49931
1	ATTN: Dr. Harold W. Lord

No. of Copies	To
	Test, Inc. 4025 Avati Drive San Diego, CA 92117
1	ATTN: Dr. Gloria Ma
	Boeing Helicopters P.O. Box 16858 Philadelphia, PA 19142
1	ATTN: A. Hans Magiso, MS P32-38
1	Glenn Rossi, MS P31-23
	Amoco Performance Products 38-C Grove Street Ridgefield, CT 06877
1	ATTN: Dr. Neil J. McCarthy
	Rockwell International P.O. Box 582808 D996, B116 Tulsa, OK 74158
1	ATTN: Robert B. Meadows
	Delsen Testing Laboratories 1024 Grand Central Avenue Glendale, CA 91201
1	ATTN: John Moylan
	The Aerospace Corporation P.O. Box 92957 Los Angeles, CA 90009
1	ATTN: Ashok Munjal
	Sundstrand Advanced Technology Gr. 4747 Harrison Ave. P.O. Box 7002 Rockford, IL 61125-7002
1	ATTN: Patrick Murray
	Huck Manufacturing 6 Thomas Irvine, CA 92718
1	ATTN: Douglas Olson
	Grumman Aircraft Systems Bethpage, NY 11714
1	ATTN: Paul Pittari, MS A04-12
1	Peter Shyprykevich, MS B4435
	General Electric Aircraft Engines 8143 Traverse Ct Cincinnati, OH 45215
1	ATTN: Raymond A. Rawlinson
	McDonnell Douglas Technologies, Inc. 16761 Via Del Camp Court San Diego, CA 92127
1	ATTN: Ken Sanger, MC B2-31

No. of Copies	To
	Boeing Computer Services P.O. Box 24346, MS 7L-22 Seattle, WA 98124-0346
1	ATTN: Dr. Fritz Scholz
	Martin Marietta Astronautics Group P.O. Box 179, MS I 9960 Denver, CO 80201
1	ATTN: Scott Schoultz
	ALCOA, ALCOA Labs ALCOA Center, PA 15656
1	ATTN: Robert Schultz
	Bell Helicopter Textron, Inc. P.O. Box 482, MS 4 Ft. Worth, TX 76101
1	ATTN: Lee Shahwan
	Rheometrics 3931 MacArthur Boulevard Newport Beach, CA 92660
1	ATTN: Ben Shepard
	Aerostructures, Inc. 1725 Jeff Davis Highway, Suite 704 Arlington, VA 22202
1	ATTN: Robert Simon
	Hi-Shear Corporation 1600 Skypark Drive Torrance, CA 90509
1	ATTN: Frank E. Smode
	Federal Aviation Administration 800 Independence Avenue, S.W. Washington, DC 20591
1	ATTN: Joseph R. Soderquist
	Monogram Aerospace Fasteners 3423 S. Garfield Avenue Los Angeles, CA 90040
1	ATTN: Ed Stencel
	Virginia Tech Center for Comp. Matls. & Struc. Blacksburg, VA 24061
1	ATTN: Dr. Wayne Stinchcomb
	Beech Aircraft Corporation Dept. 37 9709 East Central Wichita, KS 67201-0085
1	ATTN: Louis M Strunk

No. of Copies	To
	BASF-Narmco 1440 N. Kraemer Boulevard Anaheim, CA 92806
1	ATTN: Michael Stuart
	David Taylor Research Center Bethesda, MD 20084-5000
1	ATTN: Robert Tacey
	FMC Corporation Corporate Tech Center Box 580 Santa Clara, CA 95052
1	ATTN: George Thomas
	Magnatech International P.O. Box E Sinking Spring, PA 19608
1	ATTN: David L. Thun
	Pratt & Whitney 6754 Cinnamon Ct., S.W. Stuart, FL 34997
1	ATTN: Mrs. Susan Walker
	FMC Corporation 2890 De La Cruz Blvd. Santa Clara, CA 95052
1	ATTN: Erich Weerth
	BASF/Celion Carbon Fibers 11501 Steele Creek Road Charlotte, NC 28241
1	ATTN: Dale Wilson
	U.S. Army Materials Technology Laboratory Watertown, MA 02172-0001
2	ATTN: SLCMT-TML
1	Author

U.S. Army Materials Technology Laboratory,
Watertown, Massachusetts 02172-0001
A LAYERED BEAM THEORY FOR SINGLE LAP JOINTS -
Donald W. Oplinger

Technical Report MTL TR 91-23, June 1991, 44 pp -
illus-tables, D/A Project P612105.H84

AD ____________

UNCLASSIFIED
UNLIMITED DISTRIBUTION

Key Words

Stress analysis
Bonded joints
Structures

The well known analysis of the single lap joint by Goland and Reissner provided important contributions to the literature on stress analysis of adhesive joints by clarifying not only the importance of adhesive peel stresses in joint failure, but also the role of bending deflections of the joint in controlling the level of the stresses in the adhesive layer. Subsequent efforts have suggested the need for corrections to the Goland and Reissner analysis because of what have been conceived as deficiencies in the model used to describe bending deflections of the central part of the joint where a classical homogeneous beam model without shear or thickness normal deflections were used. The present paper addresses the issue through the use of a more realistic model in which adhesive layer deflections are allowed to decouple the two halves of the joint in the overlap region in the bending deflection analysis, as well as in the analysis of adhesive layer stresses where such a decoupling was allowed by Goland and Reissner. It is found that many of the predictions of the Goland and Reissner analysis are recovered in the limit of large adherend-to-adhesive layer thickness ratios, although substantial differences from the Goland and Reissner analysis can occur for relatively thin adherends.

U.S. Army Materials Technology Laboratory,
Watertown, Massachusetts 02172-0001
A LAYERED BEAM THEORY FOR SINGLE LAP JOINTS -
Donald W. Oplinger

Technical Report MTL TR 91-23, June 1991, 44 pp -
illus-tables, D/A Project P612105.H84

AD ____________

UNCLASSIFIED
UNLIMITED DISTRIBUTION

Key Words

Stress analysis
Bonded joints
Structures

The well known analysis of the single lap joint by Goland and Reissner provided important contributions to the literature on stress analysis of adhesive joints by clarifying not only the importance of adhesive peel stresses in joint failure, but also the role of bending deflections of the joint in controlling the level of the stresses in the adhesive layer. Subsequent efforts have suggested the need for corrections to the Goland and Reissner analysis because of what have been conceived as deficiencies in the model used to describe bending deflections of the central part of the joint where a classical homogeneous beam model without shear or thickness normal deflections were used. The present paper addresses the issue through the use of a more realistic model in which adhesive layer deflections are allowed to decouple the two halves of the joint in the overlap region in the bending deflection analysis, as well as in the analysis of adhesive layer stresses where such a decoupling was allowed by Goland and Reissner. It is found that many of the predictions of the Goland and Reissner analysis are recovered in the limit of large adherend-to-adhesive layer thickness ratios, although substantial differences from the Goland and Reissner analysis can occur for relatively thin adherends.

U.S. Army Materials Technology Laboratory,
Watertown, Massachusetts 02172-0001
A LAYERED BEAM THEORY FOR SINGLE LAP JOINTS -
Donald W. Oplinger

Technical Report MTL TR 91-23, June 1991, 44 pp -
illus-tables, D/A Project P612105.H84

AD ____________

UNCLASSIFIED
UNLIMITED DISTRIBUTION

Key Words

Stress analysis
Bonded joints
Structures

The well known analysis of the single lap joint by Goland and Reissner provided important contributions to the literature on stress analysis of adhesive joints by clarifying not only the importance of adhesive peel stresses in joint failure, but also the role of bending deflections of the joint in controlling the level of the stresses in the adhesive layer. Subsequent efforts have suggested the need for corrections to the Goland and Reissner analysis because of what have been conceived as deficiencies in the model used to describe bending deflections of the central part of the joint where a classical homogeneous beam model without shear or thickness normal deflections were used. The present paper addresses the issue through the use of a more realistic model in which adhesive layer deflections are allowed to decouple the two halves of the joint in the overlap region in the bending deflection analysis, as well as in the analysis of adhesive layer stresses where such a decoupling was allowed by Goland and Reissner. It is found that many of the predictions of the Goland and Reissner analysis are recovered in the limit of large adherend-to-adhesive layer thickness ratios, although substantial differences from the Goland and Reissner analysis can occur for relatively thin adherends.

U.S. Army Materials Technology Laboratory,
Watertown, Massachusetts 02172-0001
A LAYERED BEAM THEORY FOR SINGLE LAP JOINTS -
Donald W. Oplinger

Technical Report MTL TR 91-23, June 1991, 44 pp -
illus-tables, D/A Project P612105.H84

AD ____________

UNCLASSIFIED
UNLIMITED DISTRIBUTION

Key Words

Stress analysis
Bonded joints
Structures

The well known analysis of the single lap joint by Goland and Reissner provided important contributions to the literature on stress analysis of adhesive joints by clarifying not only the importance of adhesive peel stresses in joint failure, but also the role of bending deflections of the joint in controlling the level of the stresses in the adhesive layer. Subsequent efforts have suggested the need for corrections to the Goland and Reissner analysis because of what have been conceived as deficiencies in the model used to describe bending deflections of the central part of the joint where a classical homogeneous beam model without shear or thickness normal deflections were used. The present paper addresses the issue through the use of a more realistic model in which adhesive layer deflections are allowed to decouple the two halves of the joint in the overlap region in the bending deflection analysis, as well as in the analysis of adhesive layer stresses where such a decoupling was allowed by Goland and Reissner. It is found that many of the predictions of the Goland and Reissner analysis are recovered in the limit of large adherend-to-adhesive layer thickness ratios, although substantial differences from the Goland and Reissner analysis can occur for relatively thin adherends.